Engineering oxygen-independent biotin biosynthesis in Saccharomyces cerevisiae

Wronska, Anna K.; van den Broek, Marcel; Perli, Thomas; de Hulster, Erik; Pronk, Jack T.; Daran, Jean Marc

DOI
10.1016/j.ymben.2021.05.006

Publication date
2021

Document Version
Final published version

Published in
Metabolic Engineering

Metabolic Engineering 67 (2021) 88–103

Contents lists available at ScienceDirect

Metabolic Engineering

journal homepage: www.elsevier.com/locate/meteng

Engineering oxygen-independent biotin biosynthesis in *Saccharomyces cerevisiae*

Anna K. Wronska, Marcel van den Broek, Thomas Perli, Erik de Hulster, Jack T. Pronk, Jean-Marc Daran *

Department of Biotechnology, Delft University of Technology, Van der Maasweg 9, 2629, HZ, Delft, the Netherlands

ARTICLE INFO

Keywords:
Prokaryotic pathway
Biotin biosynthesis
Vitamin B7
Gene dosage
Anoxic growth

ABSTRACT

An oxygen requirement for *de novo* biotin synthesis in *Saccharomyces cerevisiae* precludes the application of biotin-prototrophic strains in anoxic processes that use biotin-free media. To overcome this issue, this study explores introduction of the oxygen-independent *Escherichia coli* biotin-biosynthesis pathway in *S. cerevisiae*. Implementation of this pathway required expression of seven *E. coli* genes involved in fatty-acid synthesis and three *E. coli* genes essential for the formation of a pimelate thioester, key precursor of biotin synthesis. A yeast strain expressing these genes readily grew in biotin-free medium, irrespective of the presence of oxygen. However, the engineered strain exhibited specific growth rates 25% lower in biotin-free media than in biotin-supplemented media. Following adaptive laboratory evolution in anoxic cultures, evolved cell lines that no longer showed this growth difference in controlled bioreactors, were characterized by genome sequencing and proteome analyses. The evolved isolates exhibited a whole-genome duplication accompanied with an alteration in the relative gene dosages of biosynthetic pathway genes. These alterations resulted in a reduced abundance of the enzymes catalyzing the first three steps of the *E. coli* biotin pathway. The evolved pathway configuration was reverse engineered in the diploid industrial *S. cerevisiae* strain Ethanol Red. The resulting strain grew at nearly the same rate in biotin-supplemented and biotin-free media non-controlled batches performed in an anaerobic chamber. This study established an unique genetic engineering strategy to enable biotin-independent anoxic growth of *S. cerevisiae* and demonstrated its portability in industrial strain backgrounds.

1. Introduction

Typical industrial substrates derived from plant biomass such as sugarcane juice, starch, and ligno-cellulosic hydrolysates are subjected to harsh physical-chemical treatments that result in lowering nutritional properties (Basso et al., 2008) by affecting stability of vitamins (Brown and Du Vigneaud, 1941; Mauri et al., 1989; Saidi and Warthesen, 1983; Schnellbaecher et al., 2019). In these substrates, biotin concentration is ranging from 10 to 80 ppb (Jackson and Macek, 1944; Pejin et al., 1996). Preloading of cells with vitamins during biomass propagation (van Dijk et al., 2020) or supplementing vitamins during fermentation showed positive impact on yeast fermentation performance (Alfenore et al., 2002; Brandberg et al., 2005, 2007) and significantly reduced occurrences of stuck wine fermentations (Bohlscheid et al., 2007; Medina et al., 2012). Thus, the estimation and the provision of the proper nutritional requirements of a microbial strain for industrial application are key points to improve robustness of a fermentation process (Hahn-Hagerdal et al., 2005). In this context, vitamin prototrophic yeast strains could be highly beneficial.

Although most *S. cerevisiae* strains harbor all genes necessary to encode all known enzymes of the biotin biosynthesis pathway, these strains are bradytroph for biotin, exhibiting very low growth on media devoid of biotin. Evolutionary engineering and rational metabolic engineering strategies led to the selection of yeast strains whose growth in biotin-free medium was as fast as the growth of the reference strain in the presence of biotin (Bracher et al., 2017; Wronska et al., 2020). But in both cases, acquisition of the biotin prototroph phenotype was restricted to the presence of oxygen (Wronska et al., 2020).

Several essential carboxylation reactions in eukaryotes and prokaryotes require biotin as a cofactor (Perli et al., 2020c). Despite its essentiality for prototrophic growth, *de novo* synthesis of biotin is restricted to bacteria and a limited number of plant and fungal species.

* Corresponding author.
E-mail addresses: a.k.wronska@tudelft.nl (A.K. Wronska), marcel.vandenbroek@tudelft.nl (M. van den Broek), t.perli@tudelft.nl (T. Perli), a.f.dehulster@tudelft.nl (E. de Hulster), j.t.pronk@tudelft.nl (J.T. Pronk), j.g.daran@tudelft.nl (J.-M. Daran).

https://doi.org/10.1016/j.ymben.2021.05.006
Received 30 March 2021; Received in revised form 17 May 2021; Accepted 23 May 2021
Available online 28 May 2021

The well-studied biochemical reactions involved in assembly of the fused heterocyclic rings of biotin are conserved among yeasts, bacteria and plants (Patton et al., 1998). This assembly pathway starts with a thioester of either coenzyme A (CoA) or acyl carrier protein (Acp) with the 7-carbon dicarboxylic acid pimelate. This thioester is then further converted in four successive enzymatic steps catalysed by 8-amino-7-oxononanoate (7-keto-8-aminopelargonic acid, KAPA) synthase (EC 2.3.1.47), 7,8-diamino-nonanoate (DAPA) synthase (EC 2.6.1.62), dethiobiotin synthetase (EC 6.3.3.3) and biotin synthase (EC 2.8.1.6) to finally yield biotin (Streit and Entcheva, 2003). Recently, a novel reaction involved in biotin synthesis was reported for cyanobacteria. In this reaction, the single-turnover suicide enzyme BioU converts KAPA to DAPA, using its Lys124 residue as an amino donor (Sakaki et al., 2020) (Fig. 1).

The pathway for synthesis of the pimeloyl thioester that contributes to the valerate side chain of biotin is much less conserved and the origin of the pimeloyl moiety in eukaryotes remains elusive. The recent characterization of Bio1 from *Cyberlindnera fabianii* and *Saccharomyces cerevisiae,* an enzyme whose activity remains unresolved but which is essential for pimeloyl-thioester formation in yeast (Hall and Dietrich, 2007), revealed that it catalyzes an oxygen-dependent reaction (Wronska et al., 2020). A similar oxygen dependency has been reported for the *Bacillus subtilis* P450-enzyme BioI (Fig. 1), which performs oxidative cleavage of ACP-bound long-chain fatty and thereby generates pimeloyl-thioester for biotin synthesis (Stok and De Voss, 2000). Expression of *C. fabianii* Bio1 conferred full biotin prototrophy to oxic cultures of multiple laboratory and industrial strains of *S. cerevisiae* (Wronska et al., 2020). However, due to the oxygen dependence of this enzyme, this strategy is not applicable in large-scale anoxic processes such as the yeast-based production of ethanol and isobutanol.

Prokaryotic metabolism offers options for pimeloyl-thioester biosynthesis that are independent of molecular oxygen and might be suitable for implementation in *S. cerevisiae* to meet biotin demands in processes performed in absence of oxygen. In *B. subtilis*, pimeloyl-CoA can be formed by BioW, a pimeloyl-CoA synthetase that converts free pimelic acid to pimeloyl-CoA in presence of ATP and free CoA (Bower et al., 1996). The substrate of BioW, pimelic acid (heptanedioic acid), has been proposed to be derived from fatty acid synthesis (Manandhar and Cronan, 2017). In *Escherichia coli*, a divergent pathway for pimelate thioester synthesis has been elucidated (Lin et al., 2010). This pathway

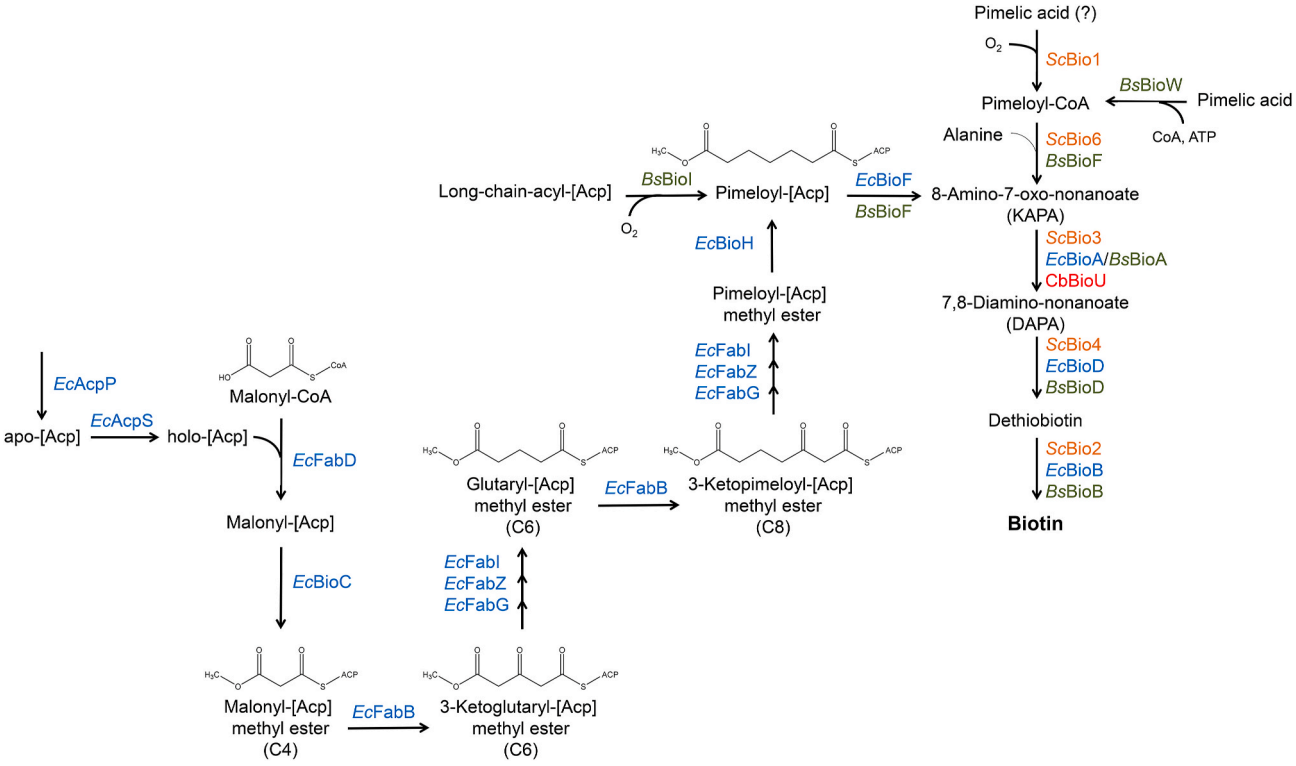

Fig. 1. Biotin biosynthesis pathways in *Escherichia coli* (blue), *Bacillus subtilis* (green), cyanobacteria (red) and yeast (orange). The *E. coli*-derived steps for biotin synthesis (blue) start from the acyl-carrier protein (AcpP), which is converted from its inactive apo-form into holo-[Acp] by the holo-[Acp] synthase AcpS. The malonyl-CoA-[Acp] protein transacylase FabD (EC 2.3.1.39) uses holo-[Acp] to attach the acyl-carrier protein to malonyl-CoA. The resulting malonyl-[Acp] receives a methyl group by SAM-dependent activity of the malonyl-[Acp] O methyltransferase BioC (EC 2.1.1.197). The four-carbon (C4) molecule is elongated by the 3-oxoacyl-[Acp] synthase FabB (EC 2.3.1.41). The enoyl-[Acp] reductase FabI (EC 1.3.1.9), 3-hydroxyl-[Acp] dehydratase FabZ (EC 4.2.1.59) and the 3-oxoacyl-[Acp] reductase FabG (EC 1.1.1.100) convert the product of this reaction to glutaryl-[Acp] methyl ester, which is in a subsequent step further elongated by FabB. The eight-carbon (C8) molecule is once more processed by FabI, FabZ and FabG. After two cycles of elongation the pimeloyl moiety is complete and the pimeloyl-[Acp] methyl ester esterase BioH (EC 3.1.1.85) enzyme activity removes the methyl group from pimeloyl-[Acp] methyl ester. The resulting pimeloyl-[Acp] enters after conversion by an 8-amino-7-oxononanoate synthase BioF (EC 2.3.1.47) to KAPA the yeast biotin synthesis (orange). The pathway is prolonged by three more enzymatic steps catalysed by the yeast enzymes adenosylmethionine-8-amino-7-oxononanoate aminotransferase Bio3 (EC 2.6.1.62), dethiobiotin synthetase Bio4 (EC 6.3.3.3) and biotin synthase Bio2 (EC 2.8.1.6) or in *E. coli* (blue) or *B. subtilis* (green) via the adenosylmethionine-8-amino-7-oxononanoate aminotransferase BioA (EC 2.6.1.62) or the (S)-8-amino-7-oxononanoate synthase BioU (EC 2.6.1.-) in cyanobacteria (red), the ATP-dependent dethiobiotin synthetase BioD (EC 6.3.3.3) and biotin synthase BioB (EC 2.8.1.6) to synthesise biotin. KAPA synthesis in yeast is proposed to start with pimelic acid, derived from an unknown source indicated with (?). Pimelic-acid conversion towards KAPA involves two enzymes in yeast, the putative pimeloyl-CoA synthetase Bio1 (EC 6.2.1.14) and the 7,8-diamino-pelargonic acid aminotransferase Bio6 (EC 2.3.1.47), with one of them involving putatively oxygen in the reaction. KAPA synthesis in *B. subtilis* (green) starts with the synthesis of a pimeloyl-thioester by either CoA-dependent conversion of pimelic acid by the 6-carboxyhexanoate CoA ligase BioW (EC 6.2.1.14) or oxygen-dependent cleavage of a long chain acyl-[Acp] by the biotin biosynthesis cytochrome 450 BioI (EC 1.14.14.46). (For interpretation of the references to colour in this figure legend, the reader is referred to the Web version of this article.)

is intertwined with fatty acid synthesis and is initiated by SAM-dependent methylation of malonyl-CoA by the malonyl-[Acp] O-methyltransferase encoded by *bioC*, yielding malonyl-CoA or malonyl-[Acp]) (Lin and Cronan, 2012). The methyl group of malonyl-CoA methyl ester mimics the methyl ends of fatty acyl chains and removes the charge of the carboxyl group. Malonyl-CoA methyl ester then undergoes two cycles of chain elongation by a modified type-II fatty acid synthesis pathway involving FabB, a 3-oxoacyl-[Acp]-synthase (EC 2.3.1.41), as well as FabI (EC 1.3.1.9), FabZ (EC 4.2.1.59) and FabG (EC 1.1.1.100), which produce methyl pimeloyl-[Acp]. In a final step, BioH, a pimeloyl-[Acp] methyl esterase, removes the methyl group from pimeloyl-[Acp] methyl ester, thus preventing further elongation (Agarwal et al., 2012). The released pimeloyl-[Acp] is then used by BioF, the first enzyme of the canonical pathway for formation of the hetero-bi-cyclic ring of biotin, which is a homolog of *S. cerevisiae* Bio6. BioF produces KAPA, which is the link between all hitherto described pathways for *de novo* syntheses of biotin. KAPA can be converted to biotin by DAPA synthase (Bio3, BioA) or, in cyanobacteria, by (S)-8-amino-7-oxononanoate synthase BioU (Sakaki et al., 2020), dethiobiotin synthetase (Bio4, BioU) and biotin synthase (Bio2, BioB) (Otsuka et al., 1988) (Fig. 1).

Since the multi-step prokaryotic pathway for biotin synthesis via malonyl-CoA methyl ester is not known to involve oxygen-requiring enzymes, its introduction into *S. cerevisiae* provides a possible strategy for *de novo* synthesis of biotin in anoxic cultures. To investigate this strategy, the *E. coli* genes encoding enzymes involved in KAPA synthesis, comprising *fabD*, *bioC*, *fabB*, *fabG*, *fabZ*, *fabI*, *bioH*, *bioF*, *acpP* and *acpS*, were expressed in *S. cerevisiae*. Individual transformants were evolved for fast growth in biotin-free medium conditions in absence of oxygen. Evolved biotin-prototrophic lineages were characterized by whole-genome re-sequencing and observed genetic changes were reverse engineered into *S. cerevisiae* Ethanol Red, a commercial yeast strain applied in industrial bioethanol production processes.

2. Materials and methods

2.1. Strains, media and maintenance

The *S. cerevisiae* strains used in this study are derived from the CEN.PK (Entian and Kotter, 2007; Salazar et al., 2017) and Ethanol Red lineages (Leaf, Lesaffre, Marcq-en-Baroeul, France) (Table 1). Yeast strains were grown on YP medium (10 g L^{-1} yeast extract [BD Biosciences, Vianen, NL], 20 g L^{-1} peptone [BD Biosciences]) or on chemically defined medium (SM) containing 3.0 g L^{-1} KH_2PO_4, 5.0 g L^{-1} $(NH_4)_2SO_4$ 0.5 g L^{-1} $MgSO_4$, 7·H_2O, 1 mL L^{-1} trace element solution, and 1 mL L^{-1} vitamin solution (0.05 g L^{-1} D-(+)-biotin, 1.0 g L^{-1} D-calcium pantothenate, 1.0 g L^{-1} nicotinic acid, 25 g L^{-1} myo-inositol, 1.0 g L^{-1} thiamine hydrochloride, 1.0 g L^{-1} pyridoxine hydrochloride, 0.2 g L^{-1} 4-aminobenzoic acid) (Verduyn et al., 1992). The pH was adjusted to 6 with 2 M KOH prior to autoclaving at 121 °C for 20 min. Vitamin solutions were sterilized by filtration and added to the sterile medium. Concentrated sugar solutions were autoclaved at 110 °C for 20 min and added to the sterile medium to give a final concentration of 20 g L^{-1} glucose (YPD and SMD). Biotin-free SM was prepared similarly, but biotin was omitted from the vitamin solution (1.0 g L^{-1} D-calcium pantothenate, 1.0 g L^{-1} nicotinic acid, 25 g L^{-1} myo-inositol, 1.0 g L^{-1} thiamine hydrochloride, 1.0 g L^{-1} pyridoxine hydrochloride, 0.2 g L^{-1} 4-aminobenzoic acid) (Bracher et al., 2017). Similarly, after autoclaving concentrated glucose solution at 110 °C for 20 min, glucose was added to biotin-free SM to a final concentration of 20 g L^{-1} (biotin-free SMD). Solid media contained 2% (w/v) Bacto agar (BD Biosciences) and, when indicated, acetamide for SMD acetamide (20 g L^{-1} glucose, 1.2 g L^{-1} acetamide, 3.0 g L^{-1} KH_2PO_4, 6.6 g L^{-1} K_2SO_4, 0.5 g L^{-1} $MgSO_4$ 7·H_2O, 1 mL L^{-1} trace element solution and 1 mL L^{-1} vitamin solution) (Solis-Escalante et al., 2013), 200 mg L^{-1} hygromycin for YPD hygromycin and 200 mg L^{-1} G418 (geneticin) for YPD geneticin. Where indicated,

Table 1
List of strains constructed and used in this study.

Strain	Genotype	Reference or source
CEN.PK113-7D	*MAT*a *MAL2-8c SUC2*	Entian and Kotter (2007)
CEN.PK-122	*MAT*a/*MATα*	Entian and Kotter (2007)
IMS0481	Single colony isolate of CEN.PK113-7D evolved in synthetic medium without biotin	Bracher et al. (2017)
IMX1859	*MAT*a *can1*Δ::*cas9*-natNT2 *Scsga1*Δ::*ScPYK1*p-*CfBIO1-ScBIO1*t	Wronska et al. (2020)
IMX585	*MAT*a *can1*Δ::*cas9*-natNT2	Mans et al. (2015)
IMX2600	*MAT*a *can1*Δ::*cas9*-natNT2	This study
IMX2035	*MAT*a *can1*Δ::*cas9*-natNT2 *Scsga1*Δ::*SkADH1*p-*EcfabD-ScADH1*t_*SkTDH2*p-*EcbioC-ScTEF2*t_*SkPDC1*p-*EcfabB-ScPYK1*t_*SkFBA1*p-*EcfabG-ScFBA1*t_*SePDC1*p-*EcfabZ-ScPDC1*t_*ScENO2*p-*EcfabI-ScPFK2*t_*ScPYK1*p-*EcbioH-ScPGI1*t_*ScPFK2*p-*EcbioF-ScTPIt_ScPGI1*p-*EcacpP-ScGPM1*t_*ScHXK2*p-*EcacpS-ScTDH3*t	This study
IMX2122	*MAT*a *can1*Δ::*cas9*-natNT2 *Scsga1*Δ::*SkADH1*p-*EcfabD-ScADH1*t_*SkTDH2*p-*EcbioC-ScTEF2*t_*SkPDC1*p-*EcfabB-ScPYK1*t_*SkFBA1*p-*EcfabG-ScFBA1*t_*SePDC1*p-*EcfabZ-ScPDC1*t_*ScENO2*p-*EcfabI-ScPFK2*t_*ScPYK1*p-*EcbioH-ScPGI1*t_*ScPFK2*p-*EcbioF-ScTPIt_ScPGI1*p-*EcacpP-ScGPM1*t_*ScHXK2*p-*EcacpS-ScTDH3*t *Scbio1*Δ	This study
IMS0994	Single colony isolate of IMX2122 evolved under anoxic conditions without biotin in bioreactor A	This study
IMS0995	Single colony isolate of IMX2122 evolved under anoxic conditions without biotin in bioreactor B	This study
Ethanol Red	*MAT*a/α (diploid prototrophic industrial bioethanol production strain)	F.R. Lesaffre
IMX2555	Ethanol Red *Scsga1*Δ::*SkADH1*p-*EcfabD-ScADH1*t_*SkTDH2*p-*EcbioC-ScTEF2*t_*SkPDC1*p-*EcfabB-ScPYK1*t_*SkFBA1*p-*EcfabG-ScFBA1*t_*SePDC1*p-*EcfabZ-ScPDC1*t_*ScENO2*p-*EcfabI-ScPFK2*t_*ScPYK1*p-*EcbioH-ScPGI1*t_*ScPFK2*p-*EcbioF-ScTPIt_ScPGI1*p-*EcacpP-ScGPM1*t_*ScHXK2*p-*EcacpS-ScTDH3*t/*Scsga1*Δ::*SkADH1*p-*EcfabD-ScADH1*t_*SkTDH2*p-*EcbioC-ScTEF2*t_*SkPDC1*p-*EcfabB-ScPYK1*t_*SkFBA1*p-*EcfabG-ScFBA1*t_*SePDC1*p-*EcfabZ-ScPDC1*t_*ScENO2*p-*EcfabI-ScPFK2*t_*ScPYK1*p-*EcbioH-ScPGI1*t_*ScPFK2*p-*EcbioF-ScTPIt_ScPGI1*p-*EcacpP-ScGPM1*t_*ScHXK2*p-*EcacpS-ScTDH3*t	This study
IMX2632	Ethanol Red *Scsga1*Δ::*SkADH1*p-*EcfabD-ScADH1*t_*SkTDH2*p-*EcbioC-ScTEF2*t_*SkPDC1*p-*EcfabB-ScPYK1*t_*SkFBA1*p-*EcfabG-ScFBA1*t_*SePDC1*p-*EcfabZ-ScPDC1*t_*ScENO2*p-*EcfabI-ScPFK2*t_*ScPYK1*p-*EcbioH-ScPGI1*t_*ScPFK2*p-*EcbioF-ScTPIt_ScPGI1*p-*EcacpP-ScGPM1*t_*ScHXK2*p-*EcacpS-ScTDH3*t/*Scsga1*Δ::*AgTEF*p-kanMX-*AgTEF*t_*SkFBA1*p-*EcfabG-ScFBA1*t_*SePDC1*p-*EcfabZ-ScPDC1*t_*ScENO2*p-*EcfabI-ScPFK2*t_*ScPYK1*p-*EcbioH-ScPGI1*t_*ScPFK2*p-*EcbioF-ScTPIt_ScPGI1*p-*EcacpP-ScGPM1*t_*ScHXK2*p-*EcacpS-ScTDH3*t	This study
IMX2706	*MAT*a *can1*Δ::*cas9*-natNT2 *Scsga1*Δ::*SkTDH2*p-*EcbioC-ScTEF2*t_*ScPYK1*p-*EcbioH-ScPGI1*t_*ScPFK2*p-*EcbioF*Δ-*ScTPI*t	This study
IMX2707	*MAT*a *can1*Δ::*cas9*-natNT2 *Scsga1*Δ::*SkADH1*p-*EcfabD-ScADH1*t_*SkTDH2*p-*EcbioC-ScTEF2*t_*SkPDC1*p-*EcfabB-ScPYK1*t_*SkFBA1*p-*EcfabG-ScFBA1*t_*SePDC1*p-*EcfabZ-ScPDC1*t_*ScENO2*p-*EcfabI-ScPFK2*t_*ScPYK1*p-*EcbioH-ScPGI1*t_*ScPFK2*p-*EcbioF*Δ-*ScTPIt_ScPGI1*p-*EcacpP-ScGPM1*t_*ScHXK2*p-*EcacpS-ScTDH3*t	This study

unsaturated fatty acids and/or sterols were added to autoclaved media as Tween 80 (polyethylene glycol sorbate monooleate, Merck, Darmstadt, Germany) and ergosterol (≥95% pure, Sigma-Aldrich, St. Louis, MO). 800-fold concentrated stock solutions of these "anaerobic" growth factors were prepared as described previously and incubated at 80 °C for 20 min before diluting them in growth medium, yielding final concentrations of 420 mg L^{-1} Tween 80 and 10 mg L^{-1} ergosterol (Dekker et al., 2019).

E. coli cells (XL1-Blue, Agilent Technologies, Santa Clara, CA) were grown in Lysogeny broth (LB) medium (5.0 g L^{-1} yeast extract, 10 g L^{-1} Bacto trypton [BD Biosciences], 5.0 g L^{-1} NaCl) supplemented with 25 mg L^{-1} chloramphenicol, 100 mg L^{-1} ampicillin or 50 mg L^{-1} kanamycin for selection. Solid LB medium contained 2% bacto agar.

Unless indicated otherwise, stock cultures for strain maintenance were prepared by growing yeast strains on YPD and *E. coli* cultures on LB with appropriate antibiotic markers. After reaching late exponential phase, cultures were complemented with sterile glycerol to a final concentration of 30% (v/v) and stored at −80 °C as 1 mL aliquots until use.

2.2. Shake flask cultivations

For cultivation experiments for determination of specific growth rates, 1 mL aliquot of a stock culture was inoculated in 100 mL SMD in a 500 mL shake flask and incubated for 20 h at 30 °C. A second 100 mL SMD culture was started by inoculating 2 mL of the first shake flask culture. When the second culture reached mid-exponential phase, which corresponded to an optical density at 660 nm (OD_{660}) of 3–5, an aliquot was used to inoculate a third culture at an OD_{660} of 0.1–0.3. For biotin-free growth studies, the pre-cultivation steps were performed in biotin-free SMD. Strains *S. cerevisiae* IMX585 and CEN.PK113-7D, which consistently failed to grow on biotin-free SMD in the third culture, were included as negative controls in all growth experiments.

Growth was monitored by measuring OD_{660} of accurately diluted culture samples of the third shake-flask culture with a Jenway 7200 Spectrophotometer (Cole-Palmer, Stone, United Kingdom). Specific growth rates were calculated from a minimum number of six data points collected during exponential growth and covering 3–4 doublings of OD_{660}. Specific growth rate was calculated using the equation $X = X_0 e^{\mu t}$ in which μ indicates the exponential growth rate. All oxic shake-flask experiments were carried out as biological duplicates in an Innova shaker incubator (New Brunswick Scientific, Edison, NJ) set at 30 °C and 200 rpm. To test if growth rate averages observed for different combinations of strains and medium composition are significantly different, one-way analyses of variance (ANOVA) and Tukey's multiple comparison test with $\alpha = 0.05$ were performed using GraphPad Prism 8.2.1 software (GraphPad Software, Inc., San Diego, CA).

For growth profiling under anoxic conditions, the first and second pre-culture were grown in 100 mL SMD or biotin-free SMD in a 500 mL shake flask as described previously. A 200 μL sample of mid-exponential-phase (OD_{660} of 3–5) cells from the second culture was then transferred to a Bactron 300 anaerobic workstation (Sheldon Manufacturing Inc., Cornelius, OR) operated at 30 °C. The gas mixture used for flushing the workspace and air lock consisted of 85% N2, 10% CO2 and 5% H2. An IKA KS 260 Basic orbital shaker platform (Dijkstra Verenigde BV, Lelystad, The Netherlands) placed in the anaerobic chamber was set at 200 rpm. A palladium catalyst for hydrogen-dependent oxygen removal was introduced into the chamber to reduce oxygen contamination. Cultures were grown in 50-mL shake flasks containing 40 mL SMD or biotin-free SMD. Concentrated solutions of ergosterol and/or Tween 80 were added as indicated. Sterile growth media were pre-incubated in the anaerobic chamber for at least 48 h prior to inoculation to allow for removal of oxygen. Growth experiments in the anaerobic chamber were started by inoculating shake flasks, containing SMD or biotin-free SMD, with 200 μL of an exponentially growing oxic pre-culture. Growth was measured by periodic measurements of the OD600 with an Ultrospec 10 cell-density meter (Biochrom, Cambridge, UK) placed inside the anaerobic chamber. Strains IMX585 and CEN.PK113-7D grown in SMD without "anaerobic" growth factors were used as controls for absence of oxygen in all anoxic experiments (Dekker et al., 2019). All shake flask experiments were carried out as biological duplicates.

2.3. Molecular biology techniques

DNA fragments were amplified by PCR amplification with Phusion Hot Start II High Fidelity Polymerase (Thermo Fisher Scientific, Landsmeer, The Netherlands) and desalted or PAGE-purified oligonucleotide primers (Sigma-Aldrich) (Table 3). For diagnostic PCR analysis DreamTaq polymerase (Thermo Fisher Scientific) was used according to manufacturers' recommendations. PCR products were separated by gel electrophoresis and, if required, purified with a Zymoclean Gel DNA Recovery kit (Zymo Research, Irvine, CA) or GenElute PCR Clean-Up kit (Sigma-Aldrich). Assembly of DNA fragments was, if not mentioned differently, by Golden Gate cloning based on the Yeast tool kit methodology (Lee et al., 2015). Yeast strains of the CEN.PK lineage were transformed by the lithium acetate (LiAc) method (Gietz and Woods, 2002). *S. cerevisiae* Ethanol Red was transformed using electroporation as previously described (Gorter de Vries et al., 2017). Electroporated cells were plated on selective YPD hygromycin or YPD geneticin (G418) agar medium. Genomic DNA of transformants was isolated using the YeaStar Genomic DNA kit (Zymo Research) or with the SDS/LiAc protocol (Looke et al., 2011). *E. coli* cells were chemically transformed (Inoue et al., 1990) and plated on selective LB agar. Plasmids from selected clones were isolated from *E. coli* with a Sigma GenElute Plasmid kit (Sigma-Aldrich) and verified by restriction analysis (Thermo Fisher Scientific) according to the manufacturer's recommendations or by diagnostic PCR.

2.4. Plasmid construction

2.4.1. Construction of part plasmids using yeast tool kit

Coding sequences of *EcfabD, EcbioC, EcfabB, EcfabG, EcfabZ, EcfabI, EcbioH, EcbioF, EcacpP* and *EcacpS* were codon optimized for expression in *S. cerevisiae* using JCat (Grote et al., 2005) and synthesized by GeneArt (Thermo Fisher Scientific). *E. coli* cells were chemically transformed with the plasmids harbouring the coding sequences together with 5′ and 3' flanks compatible with the YTK type 3 BsaI sites (Lee et al., 2015) and after selection for the antibiotic marker stored as Yeast Tool Kit type plasmids pUD671, pUD663, pUD664, pUD665, pUD666, pUD667, pUD668, pUD669, pUD661, pUD662 (Table 2).

The promoter sequence *ScPFK2*p was obtained by PCR application from genomic DNA of CEN.PK113-7D using primer pair 9630/9631. The promoter sequence was introduced in the entry vector pUD565 (Hassing et al., 2019) using BsmBI-T4 ligase directed Golden Gate cloning resulting in Yeast Tool Kit type 2 plasmids pGGkp031. Correct assembly was confirmed by restriction analysis with enzyme PvuII (Thermo Fisher Scientific) according to manufacturer's recommendations. The Yeast Tool Kit type plasmid was propagated in *E. coli* grown in liquid LB chloramphenicol at 37 °C and stored at −80 °C.

The terminator sequences *ScFBA1*t, *ScTPI1*t and *ScPGI1*t were obtained by PCR with primer combinations 10757/10758, 10765/10766 and 10771/10772, respectively using genomic DNA of *S. cerevisiae* CEN.PK113-7D as template. The terminator sequences were cloned in pUD565 using BsmBI-T4 DNA ligase directed Golden Gate cloning yielding the Yeast Tool Kit type 4 plasmids pGGkp046, pGGkp042 and pGGkp044 respectively. After assembly and transformation into *E. coli*, plasmids harbouring the terminator sequences were confirmed by restriction analysis with enzyme SspI (Thermo Fisher Scientific) according to manufacturer's recommendations. The Yeast Tool Kit type plasmids were stored in transformed *E. coli* cultures.

The promoter sequence *ScHXK2*p was synthesized by GeneArt

Table 2
List of plasmids constructed and used in this study.

Name	Characteristics	Reference or source
pGGkd015	*bla* ColE1 Gfp dropout	Hassing et al. (2019)
pGGkp028	*cat* ColE1 *ScENO2*p	Hassing et al. (2019)
pGGkp031	*cat* ColE1 *ScPFK2*p	This study
pGGkp033	*cat* ColE1 *ScPGI1*p	Hassing et al. (2019)
pGGkp037	*cat* ColE1 *ScADH1*t	Hassing et al. (2019)
pGGkp038	*cat* ColE1*ScTEF2*t	Hassing et al. (2019)
pGGkp040	*cat* ColE1 *ScPYK1*t	Hassing et al. (2019)
pGGkp041	*cat* ColE1 *ScTDH3*t	Hassing et al. (2019)
pGGkp042	*cat* ColE1 *ScTPI*t	This study
pGGkp044	*cat* ColE1 *ScPGI1*t	This study
pGGkp045	*cat* ColE1 *ScPDC1*t	Hassing et al. (2019)
pGGkp046	*cat* ColE1 *ScFBA1*t	This study
pGGkp048	*cat* ColE1 *ScGPM1*t	Hassing et al. (2019)
pGGkp062	*aphA* ColE1 *SkADH1*p	Hassing et al. (2019)
pGGkp063	*aphA* ColE1 *SkTDH3*p	Hassing et al. (2019)
pGGkp064	*aphA* ColE1 *SkPDC1*p	Hassing et al. (2019)
pGGkp065	*aphA* ColE1 *SkFBA1*p	Hassing et al. (2019)
pGGkp074	*cat* ColE1 *SePDC1*p	Hassing et al. (2019)
pGGkp096	*cat* ColE1 *ScHXK2*p	GeneArt
pGGkp103	*cat* ColE1 *ScPFK2*t	Hassing et al. (2019)
pGGkp117	*cat* ColE1 *ScPYK1*p	Wronska et al. (2020)
pUD565	*cat* ColE1 *GFP*	Hassing et al. (2019)
pUD661	*bla* ColE1 *EcacpP*	GeneArt
pUD662	*bla* ColE1 *EcacpS*	GeneArt
pUD663	*bla* ColE1 *EcbioC*	GeneArt
pUD664	*bla* ColE1 *EcfabB*	GeneArt
pUD665	*bla* ColE1 *EcfabG*	GeneArt
pUD666	*bla* ColE1 *EcfabZ*	GeneArt
pUD667	*bla* ColE1 *EcfabI*	GeneArt
pUD668	*bla* ColE1 *EcbioH*	GeneArt
pUD669	*bla* ColE1 *EcbioF*	GeneArt
pUD671	*bla* ColE1 *EcfabD*	GeneArt
pUD978	*bla* ColE1 *SkADH1p-EcfabD-ScADH1*t	This study
pUD979	*bla* ColE1 *SkTDH3p-EcbioC-ScTEF2*t	This study
pUD980	*bla* ColE1 *SkPDC1*p-*EcfabB-ScPYK1*t	This study
pUD981	*bla* ColE1 *SkFBA1*p-*EcfabG-SCfBA1*t	This study
pUD982	*bla* ColE1 *SePDC1*p-*EcfabZ-ScPDC1*t	This study
pUD983	*bla* ColE1 *ScENO2*p-*EcfabI-ScPFK2*t	This study
pUD984	*bla* ColE1 *ScPYK1*p-*EcbioH-ScPGI1*t	This study
pUD985	*bla* ColE1 *ScPFK2*p-*EcbioF-ScTPI*t	This study
pUD986	*bla* ColE1 *ScPGI1*p-*EcacpP-ScGPM1*t	This study
pUD987	*bla* ColE1 *ScHXK2*p-*EcacpS-ScTDH3*t	This study
pUDP145	*bla* ColE1 panARS(OPT) *hph* *ScTDH3*p–HH–gRNA$_{ScSGA1}$-HDV-*ScCYC1*t *AaTEF1*p-Spc*as9*$^{D147Y\ P411T}$-*ScPHO5*t	Wronska et al. (2020)
pUDR119	*bla* ColE1 2μ *amdS ScSNR52*p-gRNA$_{ScSGA1}$-*ScSUP4*t	Papapetridis et al. (2018)
pUDR244	*bla* ColE1 2μ *amdS ScSNR52*p-gRNA$_{ScBIO1}$-*ScSUP4*t	Wronska et al. (2020)
pUDR791	*bla* ColE1 2μ *amdS ScSNR52*p-gRNA$_{EcBioF}$-*ScSUP4*t	This study
pROS11	*bla* ColE1 2μ *amdS ScSNR52*p-gRNA$_{CAN1}$-*ScSUP4*t-*ScSNR52*p-gRNA$_{ADE2}$-*ScSUP4*t	Mans et al. (2015)
pROS13	*bla* ColE1 2μ kanMX *ScSNR52*p-gRNA$_{CAN1}$-*ScSUP4*t-*ScSNR52*p-gRNA$_{ADE2}$-*ScSUP4*t	Mans et al. (2015)

(Thermo Fisher Scientific) and is harboured by Yeast Tool Kit type 2 plasmid pGGkp096. The Yeast Tool Kit type plasmid was propagated in a chemically transformed *E. coli* cultures in liquid LB chloramphenicol medium grown at 37 °C on a rotary shaker and subsequently stored at −80 °C.

2.4.2. Construction of gRNA-expressing plasmid pUDR791

The gRNA$_{EcbioF}$ expressing plasmid pUDR791 was constructed *in vitro* by Gibson assembly. The linearized pROS11 plasmid, obtained by PCR with 6005/6006 was assembled with a PCR amplified fragment using primer 18409 and pROS11 as a template (Mans et al., 2015). Plasmid DNA was isolated from *E. coli* and correct assembly of plasmid pUDR791 was confirmed by diagnostic PCR with primers 18457/3841/5941.

2.4.3. Construction of expression cassettes

The *E. coli fabD* expression cassette was constructed by BsaI–T4 DNA ligase directed Golden Gate cloning combining DNA fragments with compatible overhangs from plasmids pGGkd015, pGGkp062, pUD671, pGGkp037 yielding plasmid pUD978. The next expression plasmids were constructed following a similar cloning principle. The *E. coli bioC* expression cassette was constructed by combining DNA fragments with compatible overhangs from plasmids pGGkd015, pGGkp063, pUD663, pGGkp038 yielding plasmid pUD979. The *E. coli fabB* expression cassette was constructed by combining DNA fragments with compatible overhangs from plasmids pGGkd015, pGGkp064, pUD664, pGGkp040 yielding plasmid pUD980. The *E. coli fabG* expression cassette was constructed by combining DNA fragments with compatible overhangs from plasmids pGGkd015, pGGkp065, pUD665, pGGkp046 yielding plasmid pUD981. The *E. coli fabZ* expression cassette was constructed by combining DNA fragments with compatible overhangs from plasmids pGGkd015, pGGkp074, pUD666, pGGkp045 yielding plasmid pUD982. The *E. coli fabI* expression cassette was constructed by combining DNA fragments with compatible overhangs from plasmids pGGkd015, pGGkp028, pUD667, pGGkp103 yielding plasmid pUD983. The *E. coli bioH* expression cassette was constructed by combining DNA fragments with compatible overhangs from plasmids pGGkd015, pGGkp117, pUD668, pGGkp044 yielding plasmid pUD984. The *E. coli bioF* expression cassette was constructed by combining DNA fragments with compatible overhangs from plasmids pGGkd015, pGGkp031, pUD669, pGGkp042 yielding plasmid pUD985. The *E. coli acpP* expression cassettee was constructed by combining DNA fragments with compatible overhangs from plasmids pGGkd015, pGGkp033, pUD661, pGGkp048 yielding plasmid pUD986. The *E. coli acpS* expression cassette was constructed by combining DNA fragments with compatible overhangs from plasmids pGGkd015, pGGkp096, pUD662, pGGkp041 yielding plasmid pUD987.

After assembly reaction and transformation of *E. coli* with the plasmids carrying the expression cassettes, four to eight colonies were selected for each plasmid, followed by isolation of plasmid DNA. Correct assembly was checked by diagnostic PCR primer combinations, with one primer binding outside the expression cassette and one within the gene sequence: 13483/12761 for *EcfabD,* 10320/10325 for *EcbioC,* 13483/12745 for *EcfabB,* 13483/12751 for *EcfabG,* 13483/12759 for *EcfabZ,* 13483/12763 for *EcfabI,* 10320/10325 for *EcbioH,* 13483/13283 for *EcbioF,* 10320/10325 for *EcacpP* and 13483/12749 for *EcacpS.* The obtained plasmids were stored as pUD979, pUD980, pUD981, pUD982, pUD983, pUD984, pUD985, pUD986, pUD987.

2.5. Strain construction

2.5.1. Integration of E. coli bio gene expression cassettes into S. cerevisiae

S. cerevisiae IMX2600 was constructed by homology-directed repair by assembly and integration of two cassettes containing *Spycas9* and the natNT2 marker into the *CAN1* locus as described in (Mans et al., 2015). The *EcbioC, EcbioH* and *EcbioF* expression cassettes were PCR-amplified with the following primer pairs adding 60-bp homologous sequences

Table 3
| List of primers used in this study.

Primer no.	Sequence 5' → 3'
1719	TCCATCCGGTCTTTATCGAC
7469	GGAGTTGACCGTCTTAACAG
9630	AAGCATCGTCTCATCGGTCTCAAACGTATTCTTAGTGGATAACATGCG
9631	TTATGCCGTCTCAGGTCTCACATATTTTAGGCTGGTATCTTGATTC
10320	CATGCGCGGATGACACGAAC
10325	AGTCATCCGAGCGTGTATTG
10757	AAGCATCGTCTCATCGGTCTCAATCCGTTAATTCAAATTAATTGATATAGTTTTTTAATG
10758	TTATGCCGTCTCAGGTCTCACAGCCGCGAACTCCAAAATGAGC
10765	AAGCATCGTCTCATCGGTCTCAATCCGATTAATATAATTATATAAAAATATTATCTTCTTTTC
10766	TTATGCCGTCTCAGGTCTCACAGCCGGTACACTTCTGAGTAAC
10771	AAGCATCGTCTCATCGGTCTCAATCCACAAATCGCTCTTAAATATATACC
10772	TTATGCCGTCTCAGGTCTCACAGCGAAATAGGACCTGATATCCTCC
10873	ACGTGCGGAATAGGAATCTC
11898	CGCGGAAACGGGTATTAGGG
11899	CTAGATCCGGTAAGCGACAG
12223	CCAGGTGGCGTGCTAAACTTTTATAATGTATAAAAACCACCACCTCATAAAGTTTACTGGATATCATCATTTCTGCCACAAATATATGTACTGAGTCTATACGTCAAAGTAAAAAAATAA
12224	TTATTTTTTTACTTTGACGTATAGACTCAGTACATATATTTGTGGCAGAAATGATGATATCCAGTAAACTTTATGAGGTGGTGGTTTTTATACATTATAAAAGTTTAGCACGCCACCTGG
12450	TCTGTCAGTTGGTTAAGCGCCGCTACGATTACTACACATGCCACAGACTGATCTACAATGTATCCTCCTTTTAAACAGTTGATG
12455	ACATTGCATGGAATCAGGGCCTCAATATGTGGGAGAATGCATGAGTACGCGAGCGATCCTCCTGGTCAAACTTCAGAACTAAG
12655	TTTACAATATAGTGATAATCGTGGACTAGAGCAAGATTTCAAATAAGTAACAGCAGCAAATCCGATTTCCGTGGTTGATG
12656	CCAGGGCTCAAATGGCATAAACACTGATGGAACAGGTAGCATCGAACGTGTGTCAAACGCATGTTAGCGTCAACAACAAG
12657	GGCACAGACGAATCACTGACTGATCTGTACCACTGCGTCGACATAACTTTCCAGAAGCGCGTGGGTGCGTCAACTACATC
12658	TGAGCCAGTGCATTCCATCGATGCAGATTCGCGTCCACGTAACGTATCGGAAGCATAGGCAACAATGCCAACCCCTCTAC
12659	TGTGAGCAGTCATCCACTCGGCATAAGCCTGAATTGCACCATATCCTTGGAAGCCTGGGCGAAGCTATCTTCCGGTTATG
12660	TCCTCGACGCGATGGCATATCCAGTGTGATAACGTATGAGAAGGTACTGGAAGCTACTGCAACACTAAACGAAGGCTATC
12663	CACTGCGTGTTAAGGATATGCCTAAGGATACATGACACGCATAGCTCATTAACCGGCACGTGGATAACATGCGGCATTTC
12664	GCCGCGTAGACAATAGATCACCATCTAGTTGAATCCTGAGAGACTATCTCTAATGACCCGGGTAAAGTACAGCTACATTC
12665	GCGTTTGACACACGTTCGATGCTACCTGTTCCATCAGTGTTTATGCCATTTGAGCCCTGGACACACCGAGATTCATCAAC
12666	GCGCTTCTGGAAAGTTATGTCGACGCAGTGGTACAGATCAGTCAGTGATTCGTCTGTGCCATATACATACGCTGACATGG
12667	GCCTATGCTTCCGATACGTTACGTGGACGCGAATCTGCATCGATGGAATGCACTGGCTCATCGCCATCCTGATAATCATG
12668	GCCCAGGCTTCCAAGGATATGGTGCAATTCAGGCTTATGCCGAGTGGATGACTGCTCACATTGAAATGACTCCGCAGTGG
12669	GCAGTAGCTTCCAGTACCTTCTCATACGTTATCACACTGGATATGCCATCGCGTCGAGGATTCCTTGGTTCCACTAATTC
12674	GAAAAAACTAGATCCGGTAAGCGACAGATCTTTGAATTTGTTTATAGCCGACTCTAAGTCCAGAATCGTTATCCTGGCGG
12745	AGCGTAGATAGAAGCGTCAG
12746	TCCAGTTGGTGACGTTAAGG
12747	TCAGCACCCAAGTCTTCAAC
12749	TCCAGATAGCCCATTCGTTG
12750	ACACTACGCTTGTGCTACTG
12751	GAAGCACCAGTAACCAAAGC
12752	CGAAGCTGCTTACATCACTG
12759	ATTGGCTTACCTGGGAAGTG
12760	TGCTTTGGTTGACGGTAAGG
12761	GTCAGCCAACATACCAACAG
12762	ACGAAGTTGGTCCAGGTAAG
12763	CGATACCGTAAGCGATAGAC
12764	CGCTGCTATGAACGAATTGG
13280	GGTTGCTTTGAAGCAAAGAG
13281	TTTGCCACCAGATGTTGTTC
13283	CAGATACTGGCGATCATCCG
13284	CTTGGGTGTTATCGCTAGAG
13483	TCTCCAGGACCATCTGAATC
13545	TTTGTGGCAACATAGCCAAC
13718	CCAATGAGTCTTCACATGGCGCGTGTCATGTATCCTTAGGCATATCCTTAACACGCAGTGCGGTACACTTCTGAGTAACC
13748	CGGGTCATTAGAGATAGTCTCTCAGGATTCAACTAGATGGTGATCTATTGTCTACGCGGCTTGGCAGCCATTAAACTACG
14000	AGGATCGCTCGCGTACTCATGCATTCTCCCACATATTGAGGCCCTGATTCCATGCAATGTCAGCAAATCGTCTATATCAC

(*continued on next page*)

Table 3 (*continued*)

Primer no.	Sequence 5′ → 3′
14448	CATTGTAGATCAGTCTGTGGCATGTGTAGTAATCGTAGCGGCGCTTAACCAACTGACAGACATTCTCTGCTGCTTTGTTG
17154	GCGCTGGCAGTGTTCCTGCG
17991	TCTTTCTTGTTAAAAATTTCAAGCTATACCAAGCATACAATCAACTATCTCATATACAATACGCTGCAGGTCGACAACC
17992	ATAAAATTTAAAAATATAATTCAAAAAAATAATATCTTCATTCAATCATGATTCTTTTTCTAGTGGATCTGATATCACC
18404	GAAAAAACTAGATCCGGTAAGCGACAGATCTTTGAATTTGTTTATAGCCGACTCTAAGTCCGGTACACTTCTGAGTAACC
18405	AGGATCGCTCGCGTACTCATGCATTCTCCCACATATTGAGGCCCTGATTCCATGCAATGTATATACATACGCTGACATGG
18406	TTTACAATATAGTGATAATCGTGGACTAGAGCAAGATTTCAAATAAGTAACAGCAGCAAAATGTTAGCGTCAACAACAAG
18407	GAACAATAGAACTAGATTTAGAGACTAGTTTAGCATTGGCCAAGAACTAACCATACGCATATCCGATTAATATAATTATATAAAAATATTATCTTCTTTTCTTTATATCTAGTGTTATGT
18408	ACATAACACTAGATATAAGAAAAGAAGATAATATTTTTATATAATTATTTAATCGGATATGCGTATGGTTAGTTCTTGGCCAATGCTAAACTAGTCTCTAAATCTAGTTCTATTGTTC
18409	TGCGCATGTTTCGGCGTTCGAAACTTCTCCGCAGTGAAAGATAAATGATCCTGGCAGGAGAAAATCAACGGTTTTAGAGCTAGAAATAGCAAGTTAAAATAAGGCTAGTCCGTTATCAAC
18418	CGTTGATTTTCTCCTGCCAG

(Kuijpers et al., 2013a): 18406/18405 for *EcbioC* (pUD979), 12455/12450 for *EcbioH* (pUD984) and 14448/18404 for *EcbioF* (pUD985). Targeting at the *ScSGA1* locus in IMX2600 was directed by Cas9 activity and a target-specific gRNA expressing plasmid. The strain was co-transformed with the *EcbioC, EcbioH* and *EcbioF* expression cassette fragments and the plasmid pUDR119 expressing the gRNA to target Cas9 activity to the *ScSGA1* locus (Papapetridis et al., 2018) using the LiAc transformation protocol. Transformed cells were plated on selective SMD with acetamide and incubated for 3 days at 30 °C. Genomic DNA of colonies was isolated and the desired genotype confirmed by diagnostic PCR using primer combinations 11898/13545, 13284/13281, 13280/13283 and 1719/11899. A verified clone was inoculated in 20 mL non-selective YPD for plasmid removal and incubated for 24 h at 30 °C. Cells were plated on YPD agar to obtain single colony isolates. One isolate was re-streaked on both selective medium and YPD. When no growth was observed on selective medium the respective clone was again checked by diagnostic PCR with above-mentioned primer combinations. The strain with *in vivo* assembled expression cassettes of the *E. coli bio* genes into *ScSGA1* was stored as IMX2706.

2.5.2. Integration of *E. coli* KAPA synthesis in IMX585 and Ethanol Red

Expression cassettes were PCR-amplified with the following primer pairs, thereby adding 60-bp homologous sequences (Kuijpers et al., 2013b) to enable *in vivo* assembly at the *ScSGA1* locus: 12655/12665 for *EcfabD* (pUD978), 12656/12666 for *EcbioC* (pUD979), 12657/12667 for *EcfabB* (pUD980), 12658/12668 for *EcfabG* (pUD981), 12659/12669 for *EcfabZ* (pUD982), 12660/14000 for *EcfabI* (pUD983), 12455/12450 for *EcbioH* (pUD984), 14448/13718 for *EcbioF* (pUD985), 12663/13748 for *EcacpP* (pUD986) and 12664/12674 for *EcacpS* (pUD987). The resulting expression cassettes were integrated at the *ScSGA1* locus in IMX585 and Ethanol Red, by transformation of specific gRNA encoded on plasmid pUDR119 in case of IMX585 and in case of Ethanol Red by plasmid pUDP145. Targeting at the *ScSGA1* locus in IMX585 was directed by strain-intrinsic Cas9 activity and in Ethanol Red by expression of *Spy-cas9* from plasmid pUDP145 (Juergens et al., 2018). Yeast strains were co-transformed with the respective plasmids and the *EcfabD, EcbioC, EcfabB, EcfabG, EcfabZ, EcfabI, EcbioH, EcbioF, EcacpP and EcacpS* expression cassettes using the LiAc transformation protocol. Transformed cells were plated on selective SMD with acetamide in case of IMX585 and on YPD with hygromycin in case of Ethanol Red and incubated for 3 days at 30 °C. Genomic DNA of colonies was isolated and the desired genotype confirmed by diagnostic PCR using following primer combinations 11898/12761, 12762/13545, 13284/12745, 12746/12751, 12752/12759, 12760/12763, 12764/13281, 13280/13283, 1719/12747 and 12750/11899. Single colony isolation and plasmid removal was performed as described for strain IMX2706. Strain IMX585 with *in vivo* assembled expression cassettes for *E. coli* KAPA synthesis into *ScSGA1* was stocked as IMX2035 and strain Ethanol Red with this modification as IMX2555 at −80 °C. The genome of strain IMX2035 was sequenced by Illumina technology (Illumina, San Diego, CA) to confirm mutation-free integration of the pathway genes.

2.5.3. Gene deletion

To delete the native *ScBIO1* locus in *S. cerevisiae* IMX2035, it was co-transformed with plasmid pUDR244 (Wronska et al., 2020) and a repair DNA fragment resulting from the annealing of oligo-nucleotides 12223/12224. Transformed cells were plated on selective SMD acetamide and incubated for 3 days at 30 °C. Genomic DNA of colonies was isolated and the desired genotype confirmed by diagnostic PCR using primer pair 7469/10873. A verified clone was inoculated in 20 mL non-selective YPD for plasmid removal and incubated for 24 h at 30 °C. Cells were plated on YPD agar in order to obtain single colony isolates. One isolate was re-streaked on both SMD acetamide and YPD. When no growth was observed on SMD acetamide the respective clone was once again confirmed by diagnostic PCR and stored as IMX2122. Similarly, to

delete the heterologously expressed *EcbioF* gene, strain IMX2035 was co-transformed with plasmid pUDR791 and a repair DNA fragment resulting from the annealing of the oligo-nucleotides 18407/18408. After growth on selective SMD acetamide, genotyping of the resulting colonies was carried out by diagnostic PCR with primer pair 1719/12747. After plasmid removal a single colony was isolated and stored as IMX2707.

Deletion of *EcfabD*, *EcbioC* and *EcfabB* in *S. cerevisiae* IMX2555, which was derived from the diploid *S. cerevisiae* strain Ethanol Red containing the KAPA synthesis pathway, was performed by transformation with and integration of a deletion cassette. The transformed linear DNA fragment contained 60-bp flanks homologous to the *SkADH1* promoter and the intergenic region between the *EcfabB* and *EcfabG* expressional units and the KanMX expression cassette conferring resistance to geneticin (Wach et al., 1994). The linear DNA fragment with the deletion cassette was obtained by PCR with the primer pair 17991/17992 using plasmid pROS13 as a template. Upon homologous recombination, the deletion cassette replaced one of the two copies of the three expression cassettes for *EcfabD*, *EcbioC* and *EcfabB*. Electroporated cells were plated on selective YPD G418 agar plates and incubated for 5 days at 30 °C. Genomic DNA of transformants was isolated and the desired genotype was confirmed by diagnostic PCR using following primer combinations 11898/12761, 12762/13545, 13284/12745, 11898/12562, 12751/17154. The correct clone was re-streaked on YPD agar to obtain single colony isolates. A single colony was once again confirmed by diagnostic PCR with above-mentioned primer combinations and inoculated for stocking in 20 mL non-selective YPD. The Ethanol Red strain with the integration of the KanMX cassette in the *ScSGA1* locus was stored as IMX2632.

2.6. Batch cultivation in bioreactors

Physiological characterization of *S. cerevisiae* IMX2122 (*Scbio1*Δ ↑*Ec*KAPA pathway) was performed in anoxic bioreactors (Applikon, Delft, The Netherlands) with a working volume of 1.0 L. All cultures were grown on biotin-free SMD; anoxic cultures were supplemented with sterile solutions of the "anaerobic" growth factors ergosterol (10 mg L^{-1}) and Tween 80 (420 mg L^{-1}), as well as with 0.2 g L^{-1} sterile antifoam C (Sigma-Aldrich). These conditions were maintained by sparging cultures with a gas mixture of N_2/CO_2 (90/10%, <10 ppm oxygen) at a rate of 0.5 L min^{-1}. Culture pH was maintained at 5.0 by automatic addition of 2 M KOH. All cultures were grown at a stirrer speed of 800 rpm and at a temperature of 30 °C. Oxygen diffusion in the bioreactors was minimized by using Neoprene tubing and Viton O-rings, and evaporation was minimized by cooling of outlet gas to 4 °C. Oxic conditions were maintained by sparging with pressurised air at a rate of 0.5 L min^{-1}. For bioreactor inocula, a 1 mL aliquot of a thawed stock culture of strain IMX2122 was inoculated in 100 mL biotin-free SMD in a 500 mL shake flask and incubated for 20 h at 30 °C. A second 100 mL biotin-free SMD culture was started by inoculating 2 mL of the first shake flask culture. Shake flasks were incubated at 30 °C and 200 rpm in an Innova incubator (Brunswick Scientific). When the second culture reached mid-exponential phase (OD_{660} of 3–5) it was used to inoculate the bioreactors at an OD_{660} of 0.1–0.3. Growth in the bioreactor was monitored based on the CO_2 concentration in the off-gas. Specific growth rates were calculated from CO_2 concentration values collected during exponential growth and covering 3–4 doublings. Specific growth rate was calculated using the equation $X = X_0 e^{\mu t}$ in which μ indicates the exponential growth rate. After anoxic cultures had reached a first CO_2 production peak and the CO_2 percentage in the off-gas subsequently decreased below more than 20% of the previously measured value, a computer-controlled peristaltic pump automatically removed *ca.* 90% of the culture volume, leaving *ca.* 10% as an inoculum for the next batch cultivation cycle that occurred after refilling the reactor with fresh medium. Specific growth rates in absence of oxygen were determined from the CO_2 profile after two empty-refill cycles in order to deplete "anaerobic" growth factors from the pre-cultures that were run in presence of oxygen (Dekker et al., 2019).

2.7. Laboratory evolution

Laboratory evolution of *S. cerevisiae* IMX2122 (*Scbio1*Δ ↑*Ec*KAPA pathway) for fast anoxic growth without biotin supplementation was performed in sequential-batch bioreactor cultures. Empty-refill cycles in two independent anoxic bioreactors, operated as described above, were continued until no further increase of the specific growth rate was observed for at least five consecutive batch cultivation cycles. Single-colony isolates from reactor A were obtained after 109 cycles and from reactor B after 100 cycles by plating on biotin-free SMD.

2.8. Whole-genome sequence analysis

DNA of *S. cerevisiae* strains IMX2035, IMX2122, IMS0994 and IMS0995 grown in shake-flask cultures with SMD was isolated with a Qiagen Blood & Cell Culture DNA kit (Qiagen, Germantown, MD), following manufacturer's specifications. Paired-end sequencing was performed on a 350-bp PCR-free insert library using an Illumina HiSeq PE150 sequencer (Novogene Company Limited, Hong Kong). Sequence data was mapped to the CEN.PK113-7D genome (Salazar et al., 2017), to which the sequences of the integrated expression cassettes for the heterologous genes *EcfabD, EcbioC, EcfabB, EcfabG, EcfabZ, EcfabI, EcbioH, EcbioF, EcacpP* and *EcacpS* were manually added. Data processing and chromosome copy number analysis were carried out as described previously (Bracher et al., 2017; Nijkamp et al., 2012).

2.9. Ploidy analysis by flow cytometry

For determination of ploidy, frozen aliquots of *S. cerevisiae* strains IMX2035, IMX2122 and the evolved strains IMS0994 and IMS0995 were thawed and used to inoculate 20-mL cultures on SMD (IMX2035 and IMX2122) or on biotin-free SMD (IMS0994 and IMS0995). After incubation at 30 °C until mid-exponential phase, cells were harvested, washed twice with demineralized water and stored in 70% ethanol at 4 °C. Sample preparation and staining was performed as described previously (Haase, 2003; van den Broek et al., 2015). Samples were processed using a BD Accuri C6 flow cytometer (BD Biosciences, San Jose, CA) and analysed using the FlowJo software package (Flowjo LLC, Ashland, OR). *S. cerevisiae* strains CEN.PK113-7D and CEN.PK122 were used as haploid and diploid references, respectively.

2.10. Proteome analysis

Frozen aliquots of *S. cerevisiae* strains IMX2122 (*Scbio1*Δ ↑*Ec*KAPA pathway), IMS0994 (evolution A IMX2122), and IMS0995 (evolution B IMX2122) were thawed and used to inoculate wake-up cultures in 20 mL biotin-free SMD. After overnight incubation at 30 °C, these cultures were used to inoculate two independent 100 mL cultures at a starting OD_{660} of 0.2. Once these cultures reached an OD_{660} of 4, 1 mL was collected and centrifuged at 3000 g for 5 min, yielding a cell pellet with a volume of approximately 60 μL. After protein extraction and trypsin digestion (Boonekamp et al., 2020), extracted peptides were re-suspended in 30 μL of 3% acetonitrile/0.01% trifluoroacetic acid. The peptide concentration was measured using a Nanodrop spectrophotometer (Thermo Scientific) at a wavelength of 280 nm. A total of 1 μg of sample was injected in a CapLC system (Thermo Scientific) coupled to an Orbitrap Q-exactive HF-X mass spectrometer (Thermo Scientific). First, samples were captured at a flow rate of 10 μL/min on a pre-column (μ-pre-column C18 PepMap 100, 5 μm, 100 Å) and subsequently peptides were separated on a 15 cm C18 easy spray column (PepMap RSLC C18 2 μm, 10^4 p.m., 150 μm × 15 cm) using a flow rate of 1.2 μL min^{-1}. A linear gradient from 4% to 76% acetonitrile in water was applied over 60 min. While spraying the samples into the mass spectrometer the instrument was

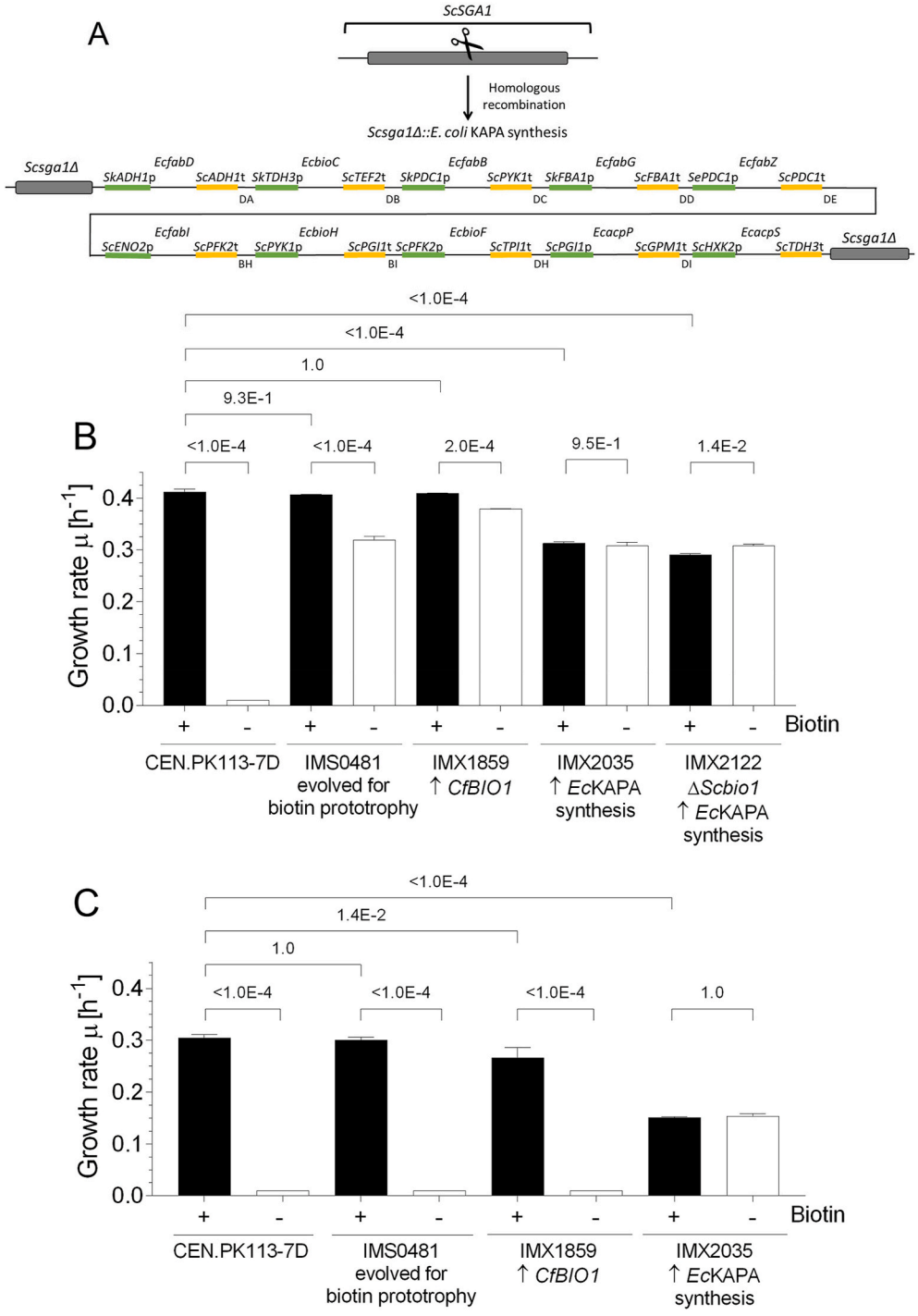

Fig. 2. Expression of *E. coli* KAPA biosynthesis pathway in *S. cerevisiae*. (A) Schematic overview of genetic modifications introduced at the *ScSGA1* locus. A Cas9-induced cut in the *ScSGA1* coding sequence and *in vivo* homologous recombination enabled integration of expression cassettes for ten *E. coli* genes with different promoters (green) and terminators (yellow). Intergenic regions consisted of synthetic 60-bp-homologous recombination sequences (Kuijpers et al., 2013b). (B) Bar graphs representing average specific growth rates of *S. cerevisiae* strains CEN.PK113-7D, IMS0481 (evolved for biotin prototrophy (Bracher et al., 2017)), IMX1859 (↑*CfBIO1* (Wronska et al., 2020),), IMX2035 (↑*Ec*KAPA pathway) and IMX2122 (*Scbio1*Δ ↑*Ec*KAPA pathway) under oxic conditions on glucose synthetic medium with (+, black) and without (-, white) biotin. (C) Bar graphs representing average specific growth rates of *S. cerevisiae* strains CEN.PK113-7D, IMS0481, IMX1859 and IMX2035 under anoxic conditions on glucose synthetic medium with (+, black) and without (-, white) biotin. Averages and deviations of the bar graphs were calculated from independent duplicate cultures. Brackets between 2 bar graphs show the p-value, which was derived from significance testing of the difference between observed growth rates by one-way analyses of variance (ANOVA) and Tukey's multiple comparison test using GraphPad prism 8.2.1 software (significance threshold $p_{\text{-value}} <$ 5.0E-02). (For interpretation of the references to colour in this figure legend, the reader is referred to the Web version of this article.)

operated in data dependent mode using settings as previously described in (Perli et al., 2021). Data analysis was performed using Proteome discover 2.4 (Thermo Scientific) with fixed modifications set to carbamidomethyl (C), variable modifications set to oxidation of methionine residues, search mass tolerance set to 20 ppm, MS/MS tolerance set to 20 ppm, trypsin selected as restriction enzyme and allowing one missed cleavage. False Discovery Rate (FDR) was set at 0.1% and the match between runs window was set to 0.7 min. Quantification was only based on unique peptides and normalization between samples was based on total peptide amount. For protein search, a protein database consisting of the *S. cerevisiae* S288C proteome amino-acid sequences together with the sequences of the heterologously expressed proteins was used. Each strain was analysed in independent biological duplicate samples. Data processing and analysis of differentially expressed proteins was conducted as previously described in (Boonekamp et al., 2020). Enrichment analysis of up- and downregulated proteins in the isolates was performed using the GO Enrichment Analysis (Mi et al., 2019).

3. Results

3.1. Expression of the E. coli KAPA-biosynthesis pathway supports biotin-independent growth of S. cerevisiae in absence of oxygen

Of the currently known prokaryotic biotin-biosynthesis pathways

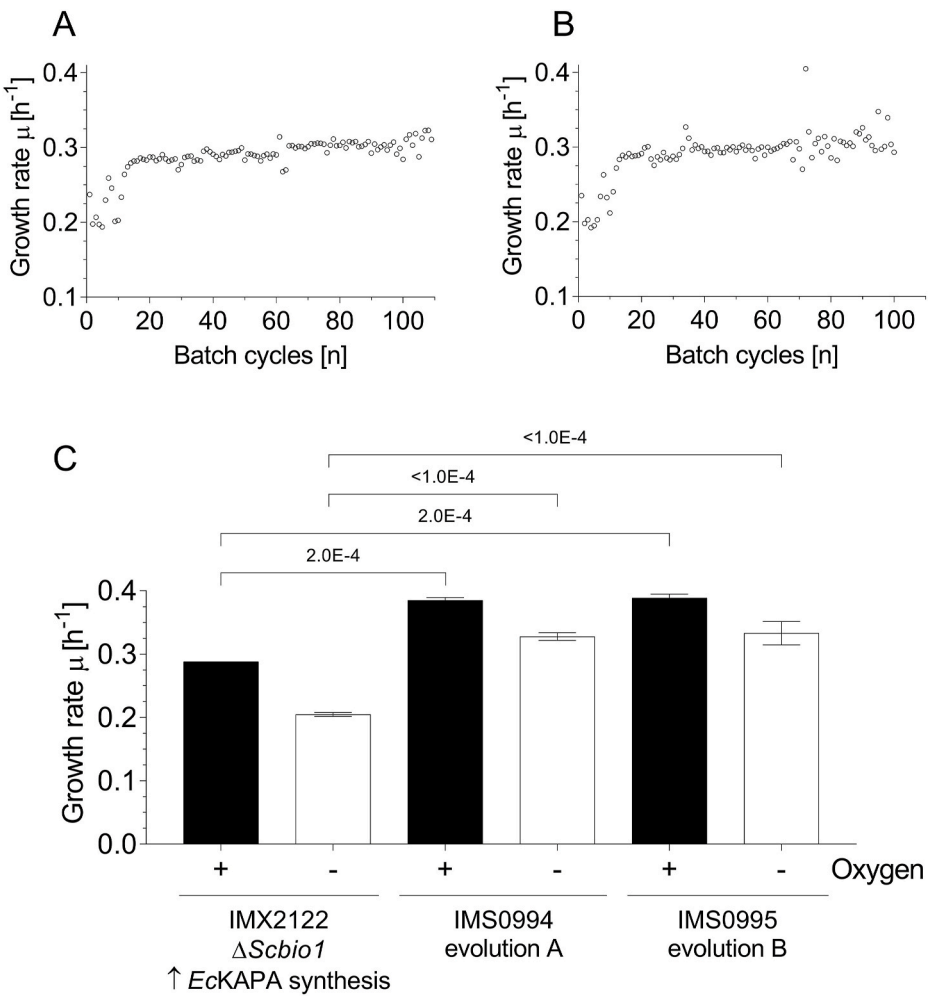

Fig. 3. Laboratory evolution of the engineered biotin-prototrophic *S. cerevisiae* strain IMX2122. (A) Specific growth rates of anoxic sequential batch cycles [n] of strain IMX2122 (*Scbio1*Δ ↑*Ec*KAPA pathway) on biotin-free medium, reactor A. (B) Specific growth rates of anoxic sequential batch cycles [n] of strain IMX2122 on biotin-free medium, reactor B. (C) Bar graphs represent average specific growth rates of the parental strain *S. cerevisiae* IMX2122 and evolved isolates IMS0994 (evolution A IMX2122) and IMS0995 (evolution B IMX2122) on synthetic medium without biotin under oxic (+, black) and anoxic (-, white) conditions. The growth rate means and deviations of the bar graphs were calculated from biological duplicates. Brackets between 2 bar graphs show the $p_{\text{-value}}$, which was derived from significance testing of the difference between observed growth rates by one-way analyses of variance (ANOVA) and Tukey's multiple comparison test using GraphPad prism 8.2.1 software (significance threshold $p_{\text{-value}} < 5.0\text{E-}02$).

(Fig. 1), only the variant that occurs in *E. coli* starts with malonyl-CoA, a key precursor for lipid synthesis in *S. cerevisiae*. To complete the malonyl-CoA conversion into pimeloyl-CoA, only *EcbioC* and *EcbioH* would be required in *S. cerevisiae* assuming that the other reactions could be performed by the native fatty acid elongation machinery. We also included *EcbioF* since it is unclear whether *Sc*Bio6, the protein ortholog of *Ec*BioF, can use pimeloyl-[Acp] as substrate. Integration of these three *E. coli* genes at the *SGA1* locus yielded *S. cerevisiae* IMX2706. Even after prolonged oxic incubation in biotin-free synthetic medium, this engineered strain did not show growth on biotin-free synthetic medium. To investigate whether this inability was related to the different organization of the prokaryotic and yeast fatty-acid-synthesis machineries, we introduced an additional set of expression cassettes for *E. coli* proteins involved in conversion of malonyl-[Acp]-methyl ester into pimeloyl-[Acp]-methyl ester. In addition to *EcbioC, H* and *F*, five genes involved in fatty-acid biosynthesis (*EcfabD, EcfabB, EcfabG, EcfabZ, EcfabI)* and two genes involved in acyl carrier protein formation *(EcacpP* and *EcacpS*) were introduced. In *E. coli,* the concerted action of the enzymes encoded by these genes converts malonyl-CoA into 8-amino-7-oxo-nonanoate (KAPA), a metabolic intermediate of the native *S. cerevisiae* biotin pathway. Using the *Spy*Cas9-expressing strain IMX585, the ten expression cassettes were integrated at the *SGA1* locus, yielding *S. cerevisiae* IMX2035 (↑*Ec*KAPA pathway; Fig. 2A). This engineered strain showed immediate oxic growth on biotin-free synthetic medium, at a specific growth rate of $0.31 \pm 0.01\ h^{-1}$. Under the same conditions, the reference strain CEN.PK113-7D was unable to grow (Bracher et al., 2017; Perli et al., 2020a; Wronska et al., 2020) (Fig. 2B).

Compared to previous *S. cerevisiae* strains engineered IMX1859 (Wronska et al., 2020), or evolved IMS0481 (Bracher et al., 2017), for biotin prototrophy, IMX2035 grew approximately 25% slower in biotin-supplemented as well as biotin-free media (Fig. 2B). However, in contrast to these other biotin-prototrophic strains, strain IMX2035 (↑*Ec*KAPA pathway) showed anoxic growth in biotin-free medium, at specific growth rate of $0.15 \pm 0.003\ h^{-1}$. Also in absence of oxygen, the specific growth rate of strain IMX2035 on biotin-supplement medium was lower than observed in cultures of reference strains (Fig. 2C). These results demonstrated that expression of the *E. coli* KAPA pathway in *S. cerevisiae* supports conversion of malonyl-CoA into KAPA and promotes biotin-independent anoxic growth of *S. cerevisiae*.

The functionality of the *Ec*KAPA pathway in *S. cerevisiae* IMX2035 enabled us to evaluate whether the orthologs *ScBIO6* and *EcbioF* are functionally redundant. To this end, *EcbioF* was deleted in strain IMX2035, yielding strain IMX2707. This deletion strain did not grow on biotin-free medium, indicating that the yeast 7,8-diamino-pelargonic acid aminotransferase *Sc*Bio6 cannot functionally replace the *E. coli* 8-amino-7-oxononanoate synthase *Ec*BioF.

3.2. Laboratory evolution for fast biotin-independent anoxic growth

To exclude the possibility that activity of the native *S. cerevisiae* biotin pathway interfered with the interpretation of results, *ScBIO1* was deleted in strain IMX2035 (↑*Ec*KAPA pathway), yielding strain IMX2122 (*Scbio1*Δ ↑*Ec*KAPA pathway). *Sc*Bio1 is proposed to catalyse an as yet unidentified reaction for synthesis of pimeloyl-CoA. In oxic cultures, strain IMX2122 showed similar specific growth rates on biotin-supplemented and biotin-free media (specific growth rates of 0.29 ±

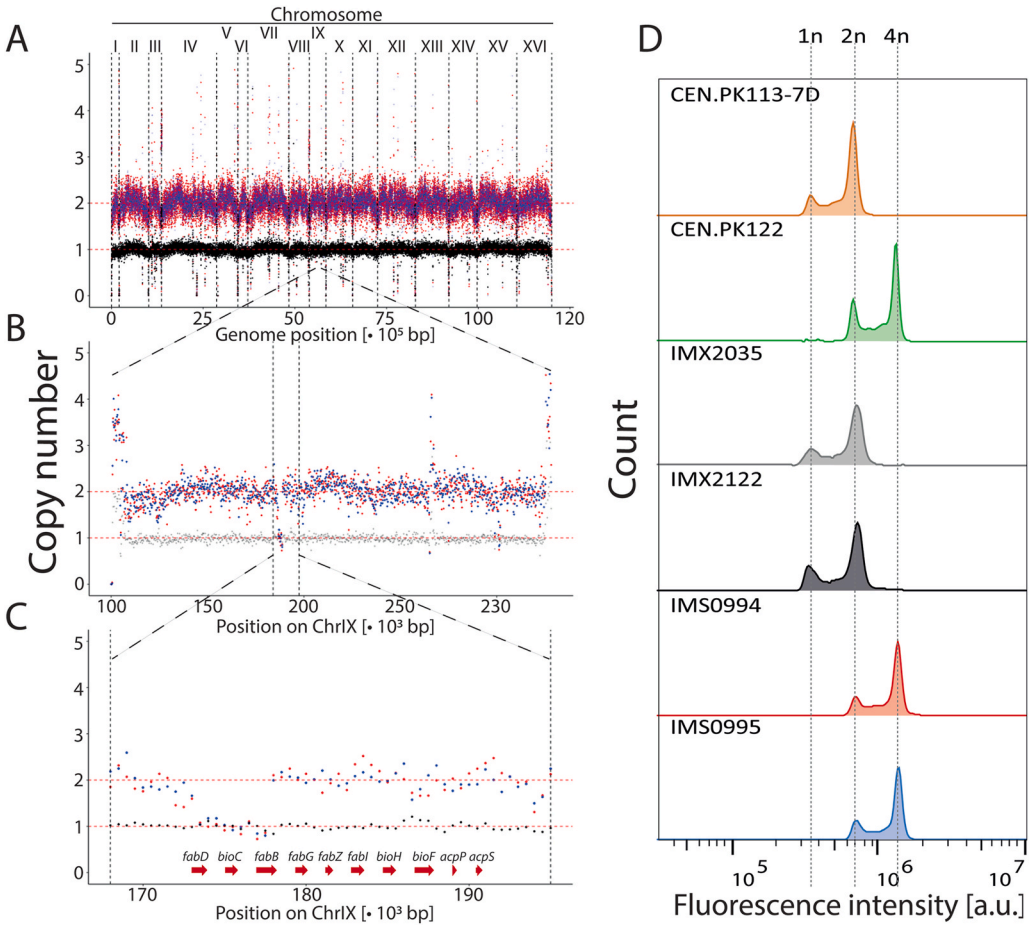

Fig. 4. Genetic alterations of the evolved isolates IMS0994 and IMS0995 compared to the initial engineered strain IMX2122. Copy number coverage plots of IMX2122 (*Scbio1*Δ ↑*Ec*KAPA pathway, black), IMS0994 (evolution A IMX2122, red) and IMS0995 (evolution B IMX2122, blue) over the whole genome (A), from position 100–250 kbp on CHRIX (B), from position 168–195 kbp on CHRIX, regions including the *E. coli* KAPA pathway *SGA1* integration site. The position of coding sequences of *E. coli* genes *fabD, bioC, fabB, fabG, fabZ, fabI, bioH, bioF, acpP* and *acpS* is indicated by red arrows (C). Histograms of fluorescence intensity of nucleic-acid-stained cells of haploid CEN.PK113-7D (orange), diploid CEN.PK122 (green), IMX2035 ((↑*Ec*KAPA pathway), grey), IMX2122 (dark grey), IMS0994 (red) and IMS0995 (blue). Vertical dashed lines indicate the fluorescence intensity of reference haploid (1n), diploid (2n) and tetraploid (4n) cells (D).

0.004 h^{-1} and 0.31 ± 0.003 h^{-1}, respectively, Fig. 2B). As anticipated, strain IMX2122 grew without oxygen on biotin-free medium, at a specific growth rate of 0.20 ± 0.001 h^{-1} (Fig. 3C). As observed for strain IMX2035 (↑*Ec*KAPA pathway) biotin supplementation did not restore the specific growth rate of strain IMX2122 to that of reference strain CEN.PK113-7D, which in both cultivation regimes on biotin-supplemented media exhibits specific growth rates of 0.32–0.33 h^{-1} (Bakker et al., 2001; Papapetridis et al., 2016) and 0.38–0.40 h^{-1} (van Maris et al., 2001),respectively.

To explore the evolvability of full biotin prototrophy, strain IMX2122 (*Scbio1*Δ ↑*Ec*KAPA pathway) was grown in two independent, anoxic sequential batch reactors (SBRs) on biotin-free synthetic medium. Throughout the course of SBR cultivation, the specific growth rate of the yeast populations in the two reactions increased to close to 0.32 h^{-1}, which corresponded closely to the reported specific growth rate on the congenic CEN.PK113-7D reference strain in absence of oxygen on chemically defined medium with biotin (Bakker et al., 2001; Papapetridis et al., 2016) (Fig. 3A and B). After 436 (109 batch cycles) and 400 generations (100 batch cycles) for reactor A and B, respectively, single colony isolates (SCI) were obtained from each reactor (IMS0994 from reactor A and IMS0995 from reactor B). Both these SCI's showed specific growth rates on biotin-free medium of 0.39 ± 0.01 h^{-1}. Under anoxic conditions, specific growth rates of the SCI's were 0.33 ± 0.01 h^{-1} and 0.33 ± 0.02 h^{-1}, respectively. These specific growth rates are virtually identical to those measured in this study for the reference strain CEN.PK113-7D during growth on biotin-containing synthetic medium under both cultivation regimes (0.41 ± 0.01 h^{-1} and 0.31 ± 0.005 h^{-1}, respectively). Compared to the specific growth rates of their parental strain IMX2122 on biotin-free medium in presence and absence of oxygen, those of the two SCI's had increased by 34% (p = 2E-04) and 57% (p = 1E-04), respectively (Fig. 3C).

3.3. Diploidization and subsequent copy-number reduction of EcKAPA biosynthesis genes contribute to evolved full biotin prototrophy

To identify the genetic basis of the evolved full prototrophy of the evolved isolates IMS0994 and IMS0995, their genomes and that of their share parental strain IMX2122 were sequenced with Illumina short-read sequencing technology and analysed. Sequence reads from the three strains were aligned with a high-quality CEN.PK113-7D genome sequence (Salazar et al., 2017) supplemented with the sequence of the contig comprising the expression cassettes of the engineered *E. coli* KAPA-pathway. Mapped data were analysed for copy number variations (CNVs), structural modifications and single nucleotide variations (SNVs) in annotated coding sequences. Prior to sequence data analysis, the nominal strain ploidy of IMX2035, IMX2122, IMS0994 and IMS0995 was analysed by nucleic acid staining and subsequent flow-cytometry analysis. The genetically engineered strains IMX2035 and IMX2122 exhibited the same ploidy as the haploid reference strain CEN.PK113-7D. In contrast, a higher fluorescence intensity of both evolved SCI's (IMS0994 and IMS0995) corresponded with that of the diploid reference strain CEN.PK122 (Fig. 4) and indicated that a whole-genome duplication had occurred in two independent evolution experiments.

CNV analysis of strains IMX2122 and IMS0994-5 did reveal a segmental aneuploidy of the engineered *SGA1* locus in which the *E. coli* KAPA pathway was integrated. As anticipated, the read coverage over the contig harbouring the *E. coli* KAPA-pathway cassettes in the parental strain IMX2122 was the same as that of the rest of the genome. In contrast, the evolved SCI's IMS0994 and IMS0995 showed a 50% lower coverage for a region comprising the three contiguous expression

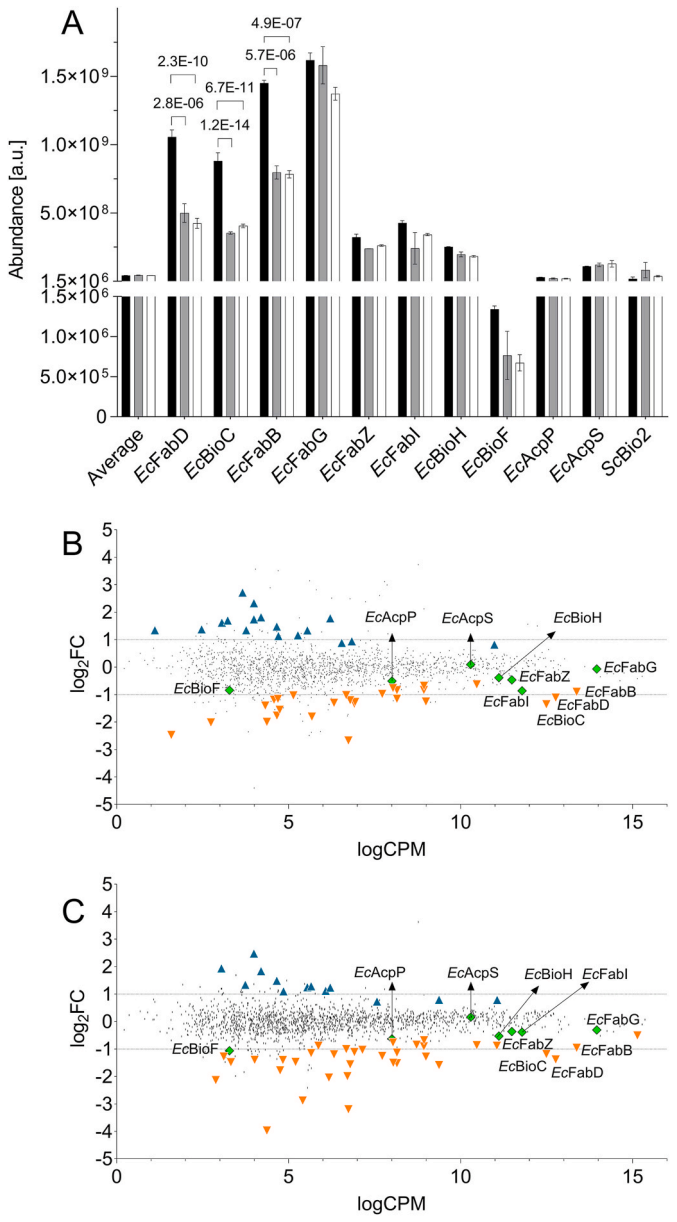

Fig. 5. Abundance of the proteins of the *Ec*KAPA pathway in IMX2122 and its derived isolates. (A) Bar graphs representing average protein abundance [a.u.] in *S. cerevisiae* strains IMX2122 ((Δ*Scbio1* ↑*Ec*KAPA pathway), black), IMS0994 (evolution A IMX2122, grey) and IMS0995 (evolution B IMX2122, white) grown in synthetic medium without biotin. The protein abundance means and deviations of *Ec*FabD, *Ec*BioC, *Ec*FabB, *Ec*FabG, *Ec*FabZ, *Ec*FabI, *Ec*BioH, *Ec*BioF, *Ec*AcpP, *Ec*AcpS and *Sc*Bio2 calculated from biological duplicates are displayed. Significance of differential expression is shown with the upper brackets and the False Discovery Rate (FDR) adjusted $p_{\text{-value}}$ ($^{\text{FDR}}p_{\text{-value}} < 5.0\text{E-}02$). (B) and (C) show dot plots representing the fold-change in protein abundance ($\log_2$FC) over the average protein concentration (logCPM) of annotated *S. cerevisiae* proteins in evolved strain IMS0994 (B) and IMS0995 (C) compared to strain IMX2122. Protein abundances with an insignificant change in expression ($^{\text{FDR}}p_{\text{-value}} > 5.0\text{E-}02$) are indicated as black dashes, protein abundances with a significant increase in expression ($^{\text{FDR}}p_{\text{-value}} < 5.0\text{E-}02$) are indicated as blue triangles and protein abundances with a significant decrease in expression ($^{\text{FDR}}p_{\text{-value}} < 5.0\text{E-}02$) are indicated as orange down-triangles (those include *Ec*FabD, *Ec*FabB and *Ec*BioC). Green diamonds represent the heterologously expressed proteins *Ec*FabG, *Ec*FabZ, *Ec*FabI, *Ec*BioH, *Ec*BioF, *Ec*AcpP and *Ec*AcpS, which were not significantly up- or downregulated.

cassettes for *EcfabD*, *EcBioC* and *EcfabB* (Fig. 4 A-B-C). This coverage reduction relative to the rest of the genome was consistent with the overall 2n ploidy of the evolved isolates (Fig. 4C and D).

While no homozygous SNVs were found in coding regions of the two evolved SCI's, a single homozygous SNV in IMS0994 was identified in the intergenic region between *PTR2* and *MLP1* on CHRXI. In addition, the two SCI's harboured a small number of heterozygous SNVs that caused amino-acid changes in the peptide sequence encoded by the mutated allele. In IMS0994 nine heterozygous SNVs occurring in coding sequences were found to be distributed over five genes (*FLO11*, *AGA1*, MFα1, *TIF3* and *ADE3*). Similarly, IMS0995 harboured ten heterozygous SNVs scattered over the coding sequences of four genes (*GLT1*, MFα1, ECM38 and *TIF3*). Out of these heterozygous SNVs, five observed in *TIF3* and one detected in MFα1 were shared by the two evolved isolates suggesting that these SNVs might originate from stock cultures used to inoculate the evolution cultures. None of the affected genes showed an obvious functional relationship with biotin-related cellular processes and the individual impact of these SNVs was not further studied.

To investigate the impact of the altered gene dosage of three *E. coli* KAPA biosynthesis genes in the evolved strains, levels of the *E. coli* KAPA pathway proteins were quantified in strains IMX2122, IMS0994 and IMS0995. Consistent with their lower copy number relative to the remainder of the genome in the evolved SCI's, abundances of the 3-oxoacyl-[Acp] synthase *Ec*FabB, the malonyl CoA-acyl carrier protein transacylase *Ec*FabD and the malonyl-[Acp] O-methyltransferase *Ec*BioC in IMS0994 and IMS0995 were at least 1.8-fold lower than those of the non-evolved parental strain IMX2122 (Fig. 5). Despite the change in ploidy, no differences in average protein abundance were observed between the three strains (Fig. 5A). While all expressed heterologous proteins were detected, *Sc*Bio2 was the only native biotin-synthesis pathway detected in the samples.

Only 44 native yeast proteins in strain IMS0994 and 48 in strain IMS0995 showed a significantly different abundance relative to the parental strain IMX2122, of which 22 showed a unidirectional difference in the two isolates (Fig. 5B and C). Not fewer than 20 and 26 proteins exhibited a 2-fold reduction at least of their abundance in IMS0994 and IMS0995 relative to IMX2122, respectively. Concomitantly, 14 and 10 proteins exhibited a 2-fold increase at least of their abundance in IMS0994 and IMS0995 relative to IMX2122, respectively (Fig. 5B and C). Proteins that showed a lower level in the two SCI's did not show GO-categories related to metabolic processes, whereas proteins that showed a higher level in IMS0994 ($^{\text{Bonferroni}}p$-value = 9.98E-07) or IMS0995 ($^{\text{Bonferroni}}p$-value = 3.41E-02) indicated an over-representation of proteins belonging to the GO-category 'ATP metabolic process' (GO:0046034). As members of this GO category, the ATP synthase subunit Atp20 as well as the cytochrome *c* oxidase subunits Cox5A and Cox13 showed higher levels in both isolates. In IMS0995, the cytochrome *c* oxidase subunit Cox4 and, in IMS0994, the cytochrome *b-c*1 complex subunit Qcr8, ATP synthase subunits Atp7 and Atp4 as well as cytochrome *c* oxidase subunit Cox9 also showed increased levels.

3.4. Reverse engineering gene dosage of the E. coli KAPA biosynthesis pathway contributes to improve both an- and oxic growth rate of the industrial diploid strain Ethanol Red

To test whether altered gene dosage of the first three genes of the oxygen-independent KAPA biosynthesis pathway relative to the downstream genes, and the corresponding lower level of the encoded proteins, was critical to enhance growth of engineered strains in biotin-free conditions, we engineered the diploid industrial strain Ethanol Red. Using CRISPR-Cas9, which enables the simultaneous modification of all gene copies in polyploid strains (Gorter de Vries et al., 2017), the ten heterologous genes were introduced at the *SGA1* locus. In contrast to the parental strain Ethanol Red, the resulting strain IMX2555 readily grew in biotin-free medium under oxic as well as under anoxic conditions. However, in both cultivation conditions, strain IMX2555 grew slower

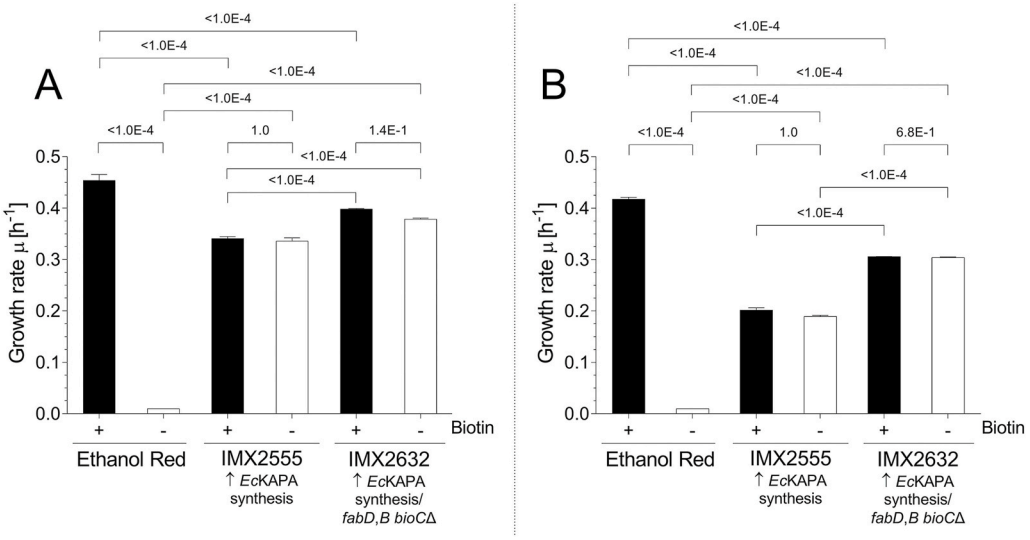

Fig. 6. | Growth of *S. cerevisiae* Ethanol Red and engineered strains expressing *E. coli* KAPA synthesis genes. (A) Bar graphs representing average specific growth rates of *S. cerevisiae* strains Ethanol Red (diploid, industrial ethanol producer), IMX2555 (Ethanol Red ↑*Ec*KAPA pathway) and IMX2632 (Ethanol Red ↑*Ec*KAPA pathway/*fabD,B bioC*Δ) under oxic conditions on synthetic medium with (+, black) and without (-, white) biotin. (B) specific growth rates of *S. cerevisiae* strains Ethanol Red, IMX2555 and IMX2632 under anoxic conditions on synthetic medium with (+, black) and without (-, white) biotin. The bars represent averages and standard deviations from two biological replicates. Statistical significance between growth rates in SMD with and without biotin, and between strains grown in the same conditions using one-way analyses of variance (ANOVA) and Tukey's multiple comparison test using GraphPad prism 8.2.1 software ($p_{\text{-value}} < 5.0E\text{-}02$) is indicated.

than Ethanol Red in biotin-supplemented medium (0.34 ± 0.01 h^{-1} versus 0.45 ± 0.01 h^{-1} and 0.20 ± 0.005 h^{-1} versus 0.42 ± 0.001 h^{-1}, respectively; Fig. 6). Specific growth rates of strain IMX2555 were not affected by the presence or absence of biotin (Fig. 6).

To reproduce the genotype observed in the evolved isolates IMS0994-5, a copy of *EcfabD, EcbioC* and *EcfabB* was deleted in IMX2555 by 'pre-CRISPR' marker-assisted homologous recombination (Wach et al., 1994) as it enables deletion of only one of the two copies of a targeted region in diploid strains. The deletion yielded the heterozygous diploid strain IMX2632 (↑*EcfabD EcbioC EcfabB,G,Z,I EcbioH,F EcacpP, S/*↑*EcfabG,Z,I EcbioH,F EcacpP,S*). The specific growth rate of strain IMX2632 in anaerobic cultures on biotin-free medium was significantly higher than that of its parental strain IMS2555 ($p_{\text{-value}} < 1.0E\text{-}04$; 0.30 ± 0.006 h^{-1} versus 0.19 ± 0.004 h^{-1}). A smaller but significantly higher specific growth rate ($p_{\text{-value}} < 1.0E\text{-}04$; 0.38 ± 0.007 h^{-1} versus 0.34 ± 0.003 h^{-1}) was observed in oxic cultures. Despite these improvements, the engineered strain IMX2632 still grew slower than observed for the Ethanol Red strain in both biotin supplemented cultures (Fig. 6), suggesting additional tuning of gene dosages of KAPA-pathway cassettes and/or other mutations are required for full anoxic biotin prototrophy in engineered strains.

4. Discussion

The native yeast pathway for biotin biosynthesis, for which the first committed reaction remains to be resolved, is oxygen dependent (Wronska et al., 2020). This study shows that functional expression of the *E. coli* KAPA pathway yields *S. cerevisiae* strains that are biotin prototrophic irrespective of the applied oxygen regime and whose specific growth rates can be further improved by tuning of the expression levels of specific KAPA-pathway enzymes.

Prokaryotic biosynthesis pathways have previously been transferred between bacteria to increase biotin production by bacterial hosts such as *Pseudomonas mutabilis* (Xiao et al., 2020), *Agrobacterium* sp. (Shaw et al., 1999) and *E. coli* (Bali et al., 2020). For functional expression of the *E. coli* KAPA pathway in *S. cerevisiae*, the different organization of prokaryotic and eukaryotic fatty-acid biosynthesis needed to be considered. In the type-II FAS system of *E. coli*, individual reactions in fatty-acid synthesis are catalysed by separate proteins (White et al., 2005). In contrast, the type-I FAS system of *S. cerevisiae* and other fungi harbours all catalytic sites required for fatty-acid biosynthesis in domains of a large, multi-functional single polypeptide or, as in *S. cerevisiae*, two polypeptides (Lomakin et al., 2007; Tehlivets et al., 2007). Despite this structural difference, functional replacement of the *S. cerevisiae* type I-FAS complex by the *E. coli* type-II FAS system has been demonstrated (Fernandez-Moya et al., 2015). In this study, expression of only *EcbioC, H* and *F* in *S. cerevisiae* did not support biotin prototrophy. This observation suggested that the yeast type-I FAS complex cannot convert malonyl-CoA methyl ester into pimeloyl-[Acp] or, alternatively, that the location of the acyl-carrier function on a distinct domain within a large multifunctional protein prevented *Ec*BioC from accessing its substrate. While the *S. cerevisiae* genome additionally encodes a soluble acyl carrier protein (Acp1) and its activating enzyme phosphopantetheine:protein transferase (Ppt2), these proteins participate in mitochondrial fatty-acid synthesis and are located in the mitochondrial matrix (Brody et al., 1997). This localization issue was circumvented by additionally expressing the *E. coli* fatty-acid synthesis genes *EcfabD,B, G, Z, I* as well as *EcacpS* and *P* and, thereby, enabling cytosolic synthesis of pimeloyl-[Acp].

In the engineered biotin-prototrophic strain IMX2035, conversion of pimeloyl-[Acp] to 7-keto-8-aminopelargonic acid (KAPA) was enabled by expression of *EcbioF*. Deletion of *EcbioF* from this strain led to loss of its biotin prototrophy. Apparently, like its *B. subtilis* ortholog BioF, *S. cerevisiae* Bio6 cannot convert pimeloyl-[Acp] to KAPA but specifically requires pimeloyl-CoA as a substrate (Manandhar and Cronan, 2018). The biotin auxotrophy of the *EcbioF* deletion strain was unlikely to be caused by an insufficient expression level of Bio6 since expression of *Sc*Bio1 or *Cf*Bio1 suffices to confer oxic biotin prototrophy in CEN.PK strains (Wronska et al., 2020).

In metabolic engineering, optimization of productivity and yield often requires balancing of the relative levels of enzymes in product pathways (Naseri and Koffas, 2020). Such balancing may be especially challenging when, as in the present study, the product pathway is strongly intertwined with core metabolic processes of the microbial host. Optimal enzyme levels can be explored by *in vitro* (Xiao et al., 2013) or *in vivo* (Lian et al., 2017; Naseri et al., 2019) approaches for combinatorial variation of the amounts of relevant enzymes. Our results illustrate how adaptive laboratory evolution (Mans et al., 2018; Sandberg et al., 2019), combined with access to a high-quality reference genome (Salazar et al., 2017), modern sequencing technologies, proteomics and a streamlined bioinformatics pipeline (Herrgard and Panagiotou, 2012; Oud et al., 2012) can provide a powerful alternative

approach to gain relevant information on pathway balancing.

Evolution of strain IMX2122 for faster biotin-independent growth involved a whole-genome duplication and subsequent reduction of the copy number of three genes of the heterologous biotin-biosynthesis pathway. Ploidy changes from haploid to diploid and from tetraploid to diploid have been reported in previous studies on evolving yeast populations subjected to strong selection pressures such as repetitive carbon-source switching (Oud et al., 2013) and ethanol stress (Voordeckers et al., 2015). A whole-genome duplication was also observed after prolonged cultivation (over 1000 generations) of haploid *S. cerevisiae* strains on complex medium (Gerstein et al., 2006). However, based on several shared homozygous and heterozygous SNVs in independently evolved isolates, we cannot exclude the possibility that a small subpopulation of diploid cells was already present in the predominantly haploid stock cultures with which the evolution experiments were inoculated.

Diploidy enabled tuning of the levels of *Ec*FabD, *Ec*BioC and *Ec*FabB relative to other KAPA pathway enzymes by gene deletion (Figs. 4 and 5). Micro-homology-mediated end joining (MMEJ), an error-prone repair mechanism that involves alignment of micro-homologous sequences before joining, is typically associated with deletions and insertions that mark the original break site. In yeast, MMEJ is enhanced by homologous flanking sequences of at least 12 nucleotides (Deng et al., 2014). Analysis of the break-point sequence in the evolved strains revealed a 18-bp (5′-CTGGTCACTCTTTGGGTG-3′) direct repeat in *EcfabD* (positions 265–283) and in *EcfabB* (positions 991 and 1009) that perfectly flanked the heterozygous deletion. This observation strongly suggests that MMEJ was responsible for the deletion (Seol et al., 2018). Deliberate introduction of short direct repeats in between clustered expression cassettes introduced into diploid or tetraploid strains by Cas9-medidated integration, followed by adaptive laboratory evolution, may be an attractive approach for exploring optimal gene dosages in heterologously expressed pathways whose *in vivo* activity can be coupled to growth or survival.

Deletion of a copy of *EcfabB, D* and *EcbioC* in the evolved diploid strains is likely to have mitigated a too strong competition for malonyl-CoA between the heterologously expressed KAPA pathway and native fatty-acid synthesis. This interpretation is consistent with the observed sub-optimal growth of the non-evolved parental strain on biotin-supplemented medium. The relevance of the segmental aneuploidy in the evolved strains was demonstrated by its reconstruction in the diploid industrial *S. cerevisiae* strain Ethanol Red. The anoxic specific growth rate of the thus engineered biotin-prototrophic strain was *ca.* 25% lower than that of biotin-supplemented cultures of non-engineered Ethanol Red. Although further targeted engineering and/or laboratory evolution is required for industrial implementation, our results demonstrate the feasibility of introducing anoxic biotin prototrophy into industrial *S. cerevisiae* strains.

Growth of wild-type *S. cerevisiae* strains on chemically defined media in absence of oxygen depends on supplementation of several nutrients, including ergosterol (Andreasen, 1953), nicotinic acid (Panozzo et al., 2002), pantothenate (Perli et al., 2020b) and biotin (Wronska et al., 2020). Although essential for fast growth, the unsaturated fatty acid requirement of *S. cerevisiae* for anoxic growth is not absolute (da Costa et al., 2018; Dekker et al., 2019). Several metabolic strategies have recently been studied to eliminate these biosynthetic oxygen requirements. Expression of a squalene-tetrahymanol cyclase gene from *Tetrahymena thermophila* was shown to enable synthesis of the sterol surrogate tetrahymanol and anoxic growth of *S. cerevisiae* in sterol-free media (Wiersma et al., 2020). Similarly, expression of fungal genes encoding an L-aspartate oxidase (NadB) and a quinolinate synthase (NadA) enabled nicotinic acid prototrophy without oxygen, while expression of heterologous L-aspartate-decarboxylases (AdcA) supported anoxic growth in the absence of pantothenate (Perli et al., 2020b). In terms of anoxic synthesis of cofactors, this leaves the puzzling case of thiamine, whose synthesis by yeast has been reported to be oxygen-dependent although the enzymes involved do not appear to require molecular oxygen (Wightman and Meacock, 2003). Further research on engineering anoxic cofactor synthesis in yeast is therefore not only relevant for the development of robust, prototrophic and feedstock-agnostic yeast strains for application in anoxic processes, but also for fundamental understanding of native biosynthetic pathways.

5. Conclusions

Functional expression of ten *E. coli* enzymes involved in KAPA synthesis enabled biotin-prototrophic growth of *S. cerevisiae* irrespective of oxygen supply. Adaptive laboratory evolution, genome resequencing, proteomics and reverse engineering of observed copy-number differences in a naive strain identified balancing of the relative levels of KAPA pathway enzymes as a key requirement for fast biotin-prototrophic growth. This metabolic engineering strategy can be used to construct *S. cerevisiae* cell factories for anoxic bioprocesses based on feedstocks with low or variable biotin contents.

Data availability

The genome sequencing data of the *S. cerevisiae* strains IMX2035, IMX2122, IMS0994 and IMS0995 can be found in the NCBI archive BioProject under the accession number PRJNA717156. The codon optimized sequences of the heterologous genes used in this study and the raw data used to draw graphs on Figs. 2, 3, 5 and 6 are available at the 4TU.Centre for research data repository (https://researchdata.4tu.nl/) under the https://doi.org/10.4121/14308007.

Funding

A.K.W., T.P. and J.-M.G.D. were supported by the European Union's Horizon 2020 research and innovation program under the Marie Skłodowska-Curie action PAcMEN (grant agreement no. 722287). J.T.P. is funded by an Advanced Grant of the European Research Council (grant no. 694633).

Declaration of interests

The authors declare the following financial interests/personal relationships which may be considered as potential competing interests: Anna Wronska, Jack T Pronk and Jean-Marc G Daran are inventors on a patent application related to this work (WO2020234215 (A1) 2020-11-26 Biotin Prototrophy). The remaining authors have no competing interests to declare.

Acknowledgments

We thank Pilar de la Torre Cortés for whole genome sequencing, Marijke Luttik for guidance during ploidy analysis, Jonna Bouwknegt, Sanne Wiersma and Wijb Dekker for instructions on anaerobic chamber experiments. We thank Tune Wulff from DTU Biosustain for the proteomics analysis. A.K.W., J.-M.G.D., and J.T.P. designed experiments. A.K.W. performed all experiments, except the proteome samples, which were prepared by T.P. E.A.F.D.H provided experimental support and valuable input on the design of bioreactor experiments. M.V.D.B. developed methods and wrote scripts for whole genome sequence and proteome analysis. A.K.W., J.-M.G.D. and J.T.P. wrote the manuscript. All authors read and commented on the manuscript and approved the final version. A.K.W., J.-M.G.D., and J.T.P. are inventors on a patent application (WO2020234215 (A1)) related to this work. The remaining authors have no competing interests to declare.

References

Agarwal, V., Lin, S., Lukk, T., Nair, S.K., Cronan, J.E., 2012. Structure of the enzyme-acyl carrier protein (ACP) substrate gatekeeper complex required for biotin synthesis. Proc. Natl. Acad. Sci. U. S. A. 109, 17406–17411.

Alfenore, S., Molina-Jouve, C., Guillouet, S.E., Uribelarrea, J.L., Goma, G., Benbadis, L., 2002. Improving ethanol production and viability of *Saccharomyces cerevisiae* by a vitamin feeding strategy during fed-batch process. Appl. Microbiol. Biotechnol. 60, 67–72.

T. J. Andreasen, A.A.S., 1953. Anaerobic nutrition of *Saccharomyces cerevisiae*. I. Ergosterol requirement for growth in a defined medium J. Cell. Physiol. 41, 23–36.

Bakker, B.M., Overkamp, K.M., van Maris, A.J., Kotter, P., Luttik, M.A., van Dijken, J.P., Pronk, J.T., 2001. Stoichiometry and compartmentation of NADH metabolism in *Saccharomyces cerevisiae*. FEMS Microbiol. Rev. 25, 15–37.

Bali, A.P., Lennox-Hvenekilde, D., Myling-Petersen, N., Buerger, J., Salomonsen, B., Gronenberg, L.S., Sommer, M.O.A., Genee, H.J., 2020. Improved biotin, thiamine, and lipoic acid biosynthesis by engineering the global regulator IscR. Metab. Eng. 60, 97–109.

Basso, L.C., de Amorim, H.V., de Oliveira, A.J., Lopes, M.L., 2008. Yeast selection for fuel ethanol production in Brazil. FEMS Yeast Res. 8, 1155–1163.

Bohlscheid, J.C., Fellman, J.K., Wang, X.D., Ansen, D., Edwards, C.G., 2007. The influence of nitrogen and biotin interactions on the performance of *Saccharomyces* in alcoholic fermentations. J. Appl. Microbiol. 102, 390–400.

Boonekamp, F.J., Dashko, S., Duiker, D., Gehrmann, T., van den Broek, M., den Ridder, M., Pabst, M., Robert, V., Abeel, T., Postma, E.D., Daran, J.M., Daran-Lapujade, P., 2020. Design and experimental evaluation of a minimal, innocuous watermarking strategy to distinguish near-identical DNA and RNA sequences. ACS Synth. Biol. 9, 1361–1375.

Bower, S., Perkins, J.B., Yocum, R.R., Howitt, C.L., Rahaim, P., Pero, J., 1996. Cloning, sequencing, and characterization of the *Bacillus subtilis* biotin biosynthetic operon. J. Bacteriol. 178, 4122–4130.

Bracher, J.M., de Hulster, E., Koster, C.C., van den Broek, M., Daran, J.G., van Maris, A.J. A., Pronk, J.T., 2017. Laboratory evolution of a biotin-requiring *Saccharomyces cerevisiae* strain for full biotin prototrophy and identification of causal mutations. Appl. Environ. Microbiol. 83. AEM.00892-17.

Brandberg, T., Karimi, K., Taherzadeh, M.J., Franzen, C.J., Gustafsson, L., 2007. Continuous fermentation of wheat-supplemented lignocellulose hydrolysate with different types of cell retention. Biotechnol. Bioeng. 98, 80–90.

Brandberg, T., Sanandaji, N., Gustafsson, L., Franzen, C.J., 2005. Continuous fermentation of undetoxified dilute acid lignocellulose hydrolysate by *Saccharomyces cerevisiae* ATCC 96581 using cell recirculation. Biotechnol. Prog. 21, 1093–1101.

Brody, S., Oh, C., Hoja, U., Schweizer, E., 1997. Mitochondrial acyl carrier protein is involved in lipoic acid synthesis in *Saccharomyces cerevisiae*. FEBS Lett. 408, 217–220.

Brown, G.B., Du Vigneaud, V., 1941. The effect of certain reagents on the activity of biotin. J. Biol. Chem. 141, 85–89.

da Costa, B.L.V., Basso, T.O., Raghavendran, V., Gombert, A.K., 2018. Anaerobiosis revisited: growth of *Saccharomyces cerevisiae* under extremely low oxygen availability. Appl. Microbiol. Biotechnol. 102, 2101–2116.

Dekker, W.J.C., Wiersma, S.J., Bouwknegt, J., Mooiman, C., Pronk, J.T., 2019. Anaerobic growth of *Saccharomyces cerevisiae* CEN.PK113-7D does not depend on synthesis or supplementation of unsaturated fatty acids. FEMS Yeast Res. 19, foz060.

Deng, S.K., Gibb, B., de Almeida, M.J., Greene, E.C., Symington, L.S., 2014. RPA antagonizes microhomology-mediated repair of DNA double-strand breaks. Nat. Struct. Mol. Biol. 21, 405–412.

Entian, K.D., Kotter, P., 2007. Yeast genetic strain and plasmid collections. Methods Microbiol. 36, 629–666.

Fernandez-Moya, R., Leber, C., Cardenas, J., Da Silva, N.A., 2015. Functional replacement of the *Saccharomyces cerevisiae* fatty acid synthase with a bacterial type II system allows flexible product profiles. Biotechnol. Bioeng. 112, 2618–2623.

Gerstein, A.C., Chun, H.J., Grant, A., Otto, S.P., 2006. Genomic convergence toward diploidy in *Saccharomyces cerevisiae*. PLoS Genet. 2, e145.

Gietz, R.D., Woods, R.A., 2002. Transformation of yeast by lithium acetate/single-stranded carrier DNA/polyethylene glycol method. Methods Enzymol. 350, 87–96.

Gorter de Vries, A.R., de Groot, P.A., van den Broek, M., Daran, J.G., 2017. CRISPR-Cas9 mediated gene deletions in lager yeast *Saccharomyces pastorianus*. Microb. Cell Factories 16, 222.

Grote, A., Hiller, K., Scheer, M., Munch, R., Nortemann, B., Hempel, D.C., Jahn, D., 2005. JCat: a novel tool to adapt codon usage of a target gene to its potential expression host. Nucleic Acids Res. 33, W526–W531.

Haase, S.B., 2003. Cell Cycle Analysis of Budding Yeast Using SYTOX Green. Curr Protoc Cytom 26, 7.23.1–7.23.4. https://doi.org/10.1002/0471142956.cy0723s26.

Hahn-Hagerdal, B., Karhumaa, K., Larsson, C.U., Gorwa-Grauslund, M., Gorgens, J., van Zyl, W.H., 2005. Role of cultivation media in the development of yeast strains for large scale industrial use. Microb. Cell Factories 4, 31.

Hall, C., Dietrich, F.S., 2007. The reacquisition of biotin prototrophy in *Saccharomyces cerevisiae* involved horizontal gene transfer, gene duplication and gene clustering. Genetics 177, 2293–2307.

Hassing, E.J., de Groot, P.A., Marquenie, V.R., Pronk, J.T., Daran, J.G., 2019. Connecting central carbon and aromatic amino acid metabolisms to improve de novo 2-phenylethanol production in *Saccharomyces cerevisiae*. Metab. Eng. 56, 165–180.

Herrgard, M., Panagiotou, G., 2012. Analyzing the genomic variation of microbial cell factories in the era of "New Biotechnology. Comput. Struct. Biotechnol. J. 3, e201210012.

Inoue, H., Nojima, H., Okayama, H., 1990. High efficiency transformation of *Escherichia coli* with plasmids. Gene 96, 23–28.

Jackson, W.R., Macek, T.J., 1944. B complex vitamins in sugar cane and sugar cane juice. Ind. Eng. Chem. 36, 261–263.

Juergens, H., Varela, J.A., Gorter de Vries, A.R., Perli, T., Gast, V.J.M., Gyurchev, N.Y., Rajkumar, A.S., Mans, R., Pronk, J.T., Morrissey, J.P., Daran, J.G., 2018. Genome editing in *Kluyveromyces* and *Ogataea* yeasts using a broad-host-range Cas9/gRNA co-expression plasmid. FEMS Yeast Res. 18.

Kuijpers, N.G., Chroumpi, S., Vos, T., Solis-Escalante, D., Bosman, L., Pronk, J.T., Daran, J.M., Daran-Lapujade, P., 2013a. One-step assembly and targeted integration of multigene constructs assisted by the I-SceI meganuclease in *Saccharomyces cerevisiae*. FEMS Yeast Res. 13, 769–781.

Kuijpers, N.G., Solis-Escalante, D., Bosman, L., van den Broek, M., Pronk, J.T., Daran, J. M., Daran-Lapujade, P., 2013b. A versatile, efficient strategy for assembly of multi-fragment expression vectors in *Saccharomyces cerevisiae* using 60 bp synthetic recombination sequences. Microb. Cell Factories 12, 47.

Lee, M.E., DeLoache, W.C., Cervantes, B., Dueber, J.E., 2015. A highly characterized yeast toolkit for modular, multipart assembly. ACS Synth. Biol. 4, 975–986.

Lian, J., HamediRad, M., Hu, S., Zhao, H., 2017. Combinatorial metabolic engineering using an orthogonal tri-functional CRISPR system. Nat. Commun. 8, 1688.

Lin, S., Cronan, J.E., 2012. The BioC O-methyltransferase catalyzes methyl esterification of malonyl-acyl carrier protein, an essential step in biotin synthesis. J. Biol. Chem. 287, 37010–37020.

Lin, S., Hanson, R.E., Cronan, J.E., 2010. Biotin synthesis begins by hijacking the fatty acid synthetic pathway. Nat. Chem. Biol. 6, 682–688.

Lomakin, I.B., Xiong, Y., Steitz, T.A., 2007. The crystal structure of yeast fatty acid synthase, a cellular machine with eight active sites working together. Cell 129, 319–332.

Looke, M., Kristjuhan, K., Kristjuhan, A., 2011. Extraction of genomic DNA from yeasts for PCR-based applications. Biotechniques 50, 325.

Manandhar, M., Cronan, J.E., 2017. Pimelic acid, the first precursor of the *Bacillus subtilis* biotin synthesis pathway, exists as the free acid and is assembled by fatty acid synthesis. Mol. Microbiol. 104, 595–607.

Manandhar, M., Cronan, J.E., 2018. A canonical biotin synthesis enzyme, 8-amino-7-oxononanoate synthase (BioF), utilizes different acyl chain donors in *Bacillus subtilis* and *Escherichia coli*. Appl. Environ. Microbiol. 84.

Mans, R., Daran, J.G., Pronk, J.T., 2018. Under pressure: evolutionary engineering of yeast strains for improved performance in fuels and chemicals production. Curr. Opin. Biotechnol. 50, 47–56.

Mans, R., van Rossum, H.M., Wijsman, M., Backx, A., Kuijpers, N.G., van den Broek, M., Daran-Lapujade, P., Pronk, J.T., van Maris, A.J., Daran, J.M., 2015. CRISPR/Cas9: a molecular Swiss army knife for simultaneous introduction of multiple genetic modifications in *Saccharomyces cerevisiae*. FEMS Yeast Res. 15 fov004.

Mauri, L.M., Alzamora, S.M., Chirife, J., Tomio, M.J., 1989. Review: kinetic parameters for thiamine degradation in foods and model solutions of high water activity. Int. J. Food Sci. Technol. 24, 1–9.

Medina, K., Boido, E., Dellacassa, E., Carrau, F., 2012. Growth of non-*Saccharomyces* yeasts affects nutrient availability for *Saccharomyces cerevisiae* during wine fermentation. Int. J. Food Microbiol. 157, 245–250.

Mi, H., Muruganujan, A., Ebert, D., Huang, X., Thomas, P.D., 2019. PANTHER version 14: more genomes, a new PANTHER GO-slim and improvements in enrichment analysis tools. Nucleic Acids Res. 47, D419–D426.

Naseri, G., Behrend, J., Rieper, L., Mueller-Roeber, B., 2019. COMPASS for rapid combinatorial optimization of biochemical pathways based on artificial transcription factors. Nat. Commun. 10, 2615.

Naseri, G., Koffas, M.A.G., 2020. Application of combinatorial optimization strategies in synthetic biology. Nat. Commun. 11, 2446.

Nijkamp, J.F., van den Broek, M.A., Geertman, J.M., Reinders, M.J., Daran, J.M., de Ridder, D., 2012. *De novo* detection of copy number variation by co-assembly. Bioinformatics 28, 3195–3202.

Otsuka, A.J., Buoncristiani, M.R., Howard, P.K., Flamm, J., Johnson, C., Yamamoto, R., Uchida, K., Cook, C., Ruppert, J., Matsuzaki, J., 1988. The *Escherichia coli* biotin biosynthetic enzyme sequences predicted from the nucleotide sequence of the bio operon. J. Biol. Chem. 263, 19577–19585.

Oud, B., Guadalupe-Medina, V., Nijkamp, J.F., de Ridder, D., Pronk, J.T., van Maris, A.J., Daran, J.M., 2013. Genome duplication and mutations in *ACE2* cause multicellular, fast-sedimenting phenotypes in evolved *Saccharomyces cerevisiae*. Proc. Natl. Acad. Sci. U. S. A. 110, E4223–E4231.

Oud, B., van Maris, A.J., Daran, J.M., Pronk, J.T., 2012. Genome-wide analytical approaches for reverse metabolic engineering of industrially relevant phenotypes in yeast. FEMS Yeast Res. 12, 183–196.

Panozzo, C., Nawara, M., Suski, C., Kucharczyka, R., Skoneczny, M., Becam, A.M., Rytka, J., Herbert, C.J., 2002. Aerobic and anaerobic NAD^+ metabolism in *Saccharomyces cerevisiae*. FEBS Lett. 517, 97–102.

Papapetridis, I., Goudriaan, M., Vazquez Vitali, M., de Keijzer, N.A., van den Broek, M., van Maris, A.J.A., Pronk, J.T., 2018. Optimizing anaerobic growth rate and fermentation kinetics in *Saccharomyces cerevisiae* strains expressing Calvin-cycle enzymes for improved ethanol yield. Biotechnol. Biofuels 11, 17.

Papapetridis, I., van Dijk, M., Dobbe, A.P., Metz, B., Pronk, J.T., van Maris, A.J., 2016. Improving ethanol yield in acetate-reducing *Saccharomyces cerevisiae* by cofactor engineering of 6-phosphogluconate dehydrogenase and deletion of *ALD6*. Microb. Cell Factories 15, 67.

Patton, D.A., Schetter, A.L., Franzmann, L.H., Nelson, K., Ward, E.R., Meinke, D.W., 1998. An embryo-defective mutant of *Arabidopsis* disrupted in the final step of biotin synthesis. Plant Physiol. 116, 935–946.

Pejin, D., DoŠEnoviĆ, I., Razmovski, R., KaradŽIĆ, V., GrbiĆ, J., 1996. Dependence of biotin content on molasses composition. J. Food Qual. 19, 353–361.

Perli, T., Moonen, D.P.I., van den Broek, M., Pronk, J.T., Daran, J.M., 2020a. Adaptive laboratory evolution and reverse engineering of single-vitamin prototrophies in *Saccharomyces cerevisiae*. Appl. Environ. Microbiol. 86.

Perli, T., van der Vorm, D.N.A., Wassink, M., van den Broek, M., Pronk, J.T., Daran, J.M., 2021. Engineering heterologous molybdenum-cofactor-biosynthesis and nitrate-assimilation pathways enables nitrate utilization by *Saccharomyces cerevisiae*. Metab. Eng. 65, 11–29.

Perli, T., Vos, A.M., Bouwknegt, J., Dekker, W.J.C., Wiersma, S.J., Mooiman, C., Ortiz-Merino, R.A., Daran, J.-M.G., Pronk, J.T., 2020b. Identification of oxygen-independent pathways for pyridine-nucleotide and Coenzyme-A synthesis in anaerobic fungi by expression of candidate genes in yeast. bioRxiv. https://doi.org/10.1101/2020.07.06.189415.

Perli, T., Wronska, A.K., Ortiz-Merino, R.A., Pronk, J.T., Daran, J.M., 2020c. Vitamin requirements and biosynthesis in *Saccharomyces cerevisiae*. Yeast 37, 283–304.

Saidi, B., Warthesen, J.J., 1983. Influence of pH and light on the kinetics of vitamin B_6 degradation. J. Agric. Food Chem. 31, 876–880.

Sakaki, K., Ohishi, K., Shimizu, T., Kobayashi, I., Mori, N., Matsuda, K., Tomita, T., Watanabe, H., Tanaka, K., Kuzuyama, T., Nishiyama, M., 2020. A suicide enzyme catalyzes multiple reactions for biotin biosynthesis in Cyanobacteria. Nat. Chem. Biol. 16, 415–422.

Salazar, A.N., Gorter de Vries, A.R., van den Broek, M., Wijsman, M., de la Torre Cortes, P., Brickwedde, A., Brouwers, N., Daran, J.G., Abeel, T., 2017. Nanopore sequencing enables near-complete *de novo* assembly of *Saccharomyces cerevisiae* reference strain CEN.PK113-7D. FEMS Yeast Res. 17, fox074.

Sandberg, T.E., Salazar, M.J., Weng, L.L., Palsson, B.O., Feist, A.M., 2019. The emergence of adaptive laboratory evolution as an efficient tool for biological discovery and industrial biotechnology. Metab. Eng. 56, 1–16.

Schnellbaecher, A., Binder, D., Bellmaine, S., Zimmer, A., 2019. Vitamins in cell culture media: stability and stabilization strategies. Biotechnol. Bioeng. 116, 1537–1555.

Seol, J.H., Shim, E.Y., Lee, S.E., 2018. Microhomology-mediated end joining: good, bad and ugly. Mutat. Res. 809, 81–87.

Shaw, N., Lehner, B., Fuhrmann, M., Kulla, H., Brass, J., Birch, O., Tinschert, A., Venetz, D., Venetz, V.V., Sanchez, J.C., Tonella, L., Hochstrasser, D., 1999. Biotin production under limiting growth conditions by *Agrobacterium/Rhizobium* HK4 transformed with a modified *Escherichia coli bio* operon. J. Ind. Microbiol. Biotechnol. 22, 590–599.

Solis-Escalante, D., Kuijpers, N.G., Bongaerts, N., Bolat, I., Bosman, L., Pronk, J.T., Daran, J.M., Daran-Lapujade, P., 2013. amdSYM, a new dominant recyclable marker cassette for Saccharomyces cerevisiae. FEMS Yeast Res. 13, 126–139.

Stok, J.E., De Voss, J., 2000. Expression, purification, and characterization of BioI: a carbon-carbon bond cleaving cytochrome P450 involved in biotin biosynthesis in *Bacillus subtilis*. Arch. Biochem. Biophys. 384, 351–360.

Streit, W.R., Entcheva, P., 2003. Biotin in microbes, the genes involved in its biosynthesis, its biochemical role and perspectives for biotechnological production. Appl. Microbiol. Biotechnol. 61, 21–31.

Tehlivets, O., Scheuringer, K., Kohlwein, S.D., 2007. Fatty acid synthesis and elongation in yeast. Biochim. Biophys. Acta 1771, 255–270.

van den Broek, M., Bolat, I., Nijkamp, J.F., Ramos, E., Luttik, M.A., Koopman, F., Geertman, J.M., de Ridder, D., Pronk, J.T., Daran, J.M., 2015. Chromosomal copy number variation in *Saccharomyces pastorianus* is evidence for extensive genome dynamics in industrial lager brewing strains. Appl. Environ. Microbiol. 81, 6253–6267.

van Dijk, M., Mierke, F., Nygard, Y., Olsson, L., 2020. Nutrient-supplemented propagation of *Saccharomyces cerevisiae* improves its lignocellulose fermentation ability. Amb. Express 10, 157.

van Maris, A.J., Bakker, B.M., Brandt, M., Boorsma, A., Teixeira de Mattos, M.J., Grivell, L.A., Pronk, J.T., Blom, J., 2001. Modulating the distribution of fluxes among respiration and fermentation by overexpression of *HAP4* in *Saccharomyces cerevisiae*. FEMS Yeast Res. 1, 139–149.

Verduyn, C., Postma, E., Scheffers, W.A., Van Dijken, J.P., 1992. Effect of benzoic acid on metabolic fluxes in yeasts: a continuous-culture study on the regulation of respiration and alcoholic fermentation. Yeast 8, 501–517.

Voordeckers, K., Kominek, J., Das, A., Espinosa-Cantu, A., De Maeyer, D., Arslan, A., Van Pee, M., van der Zande, E., Meert, W., Yang, Y., Zhu, B., Marchal, K., DeLuna, A., Van Noort, V., Jelier, R., Verstrepen, K.J., 2015. Adaptation to high ethanol reveals complex evolutionary pathways. PLoS Genet. 11, e1005635.

Wach, A., Brachat, A., Pohlmann, R., Philippsen, P., 1994. New heterologous modules for classical or PCR-based gene disruptions in *Saccharomyces cerevisiae*. Yeast 10, 1793–1808.

White, S.W., Zheng, J., Zhang, Y.M., Rock, 2005. The structural biology of type II fatty acid biosynthesis. Annu. Rev. Biochem. 74, 791–831.

Wiersma, S.J., Mooiman, C., Giera, M., Pronk, J.T., 2020. Squalene-tetrahymanol cyclase expression enables sterol-independent growth of *Saccharomyces cerevisiae*. Appl. Environ. Microbiol. 86.

Wightman, R., Meacock, P.A., 2003. The *THI5* gene family of *Saccharomyces cerevisiae:* distribution of homologues among the hemiascomycetes and functional redundancy in the aerobic biosynthesis of thiamin from pyridoxine. Microbiology (Read.) 149, 1447–1460.

Wronska, A.K., Haak, M.P., Geraats, E., Bruins Slot, E., van den Broek, M., Pronk, J.T., Daran, J.M., 2020. Exploiting the diversity of saccharomycotina yeasts to engineer biotin-independent growth of *Saccharomyces cerevisiae*. Appl. Environ. Microbiol. 86. AEM.00270-20.

Xiao, F., Wang, H., Shi, Z., Huang, Q., Huang, L., Lian, J., Cai, J., Xu, Z., 2020. Multi-level metabolic engineering of *Pseudomonas mutabilis* ATCC31014 for efficient production of biotin. Metab. Eng. 61, 406–415.

Xiao, X., Yu, X., Khosla, C., 2013. Metabolic flux between unsaturated and saturated fatty acids is controlled by the FabA:FabB ratio in the fully reconstituted fatty acid biosynthetic pathway of *Escherichia coli*. Biochemistry 52, 8304–8312.